Accepted Manuscript

Synthesis and Biological Evaluation of 1-Benzyl-*N*-(2-(phenylamino)pyridin-3-yl)-1*H*-1,2,3-triazole-4-carboxamides as Antimitotic Agents

Budaganaboyina Prasad, V. Lakshma Nayak, P.S. Srikanth, Mirza Feroz Baig, N.V. Subba Reddy, Korrapati Suresh Babu, Ahmed Kamal
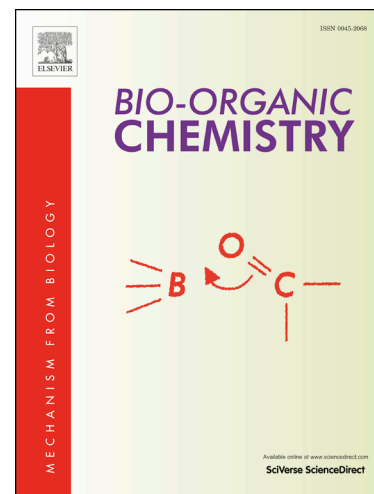
Please cite this article as: B. Prasad, V. Lakshma Nayak, P.S. Srikanth, M. Feroz Baig, N.V. Subba Reddy, K. Suresh Babu, A. Kamal, Synthesis and Biological Evaluation of 1-Benzyl-*N*-(2-(phenylamino)pyridin-3-yl)-1*H*-1,2,3-triazole-4-carboxamides as Antimitotic Agents, *Bioorganic Chemistry* (2018), doi: https://doi.org/10.1016/j.bioorg.2018.11.002

Synthesis and Biological Evaluation of 1-Benzyl-*N*-(2-(phenylamino)pyridin-3-yl)-1*H*-1,2,3-triazole-4-carboxamides as Antimitotic Agents

Budaganaboyina Prasad,[a,b] V. Lakshma Nayak,[a] P. S. Srikanth,[a] Mirza Feroz Baig,[a] N. V. Subba Reddy,[a] Korrapati Suresh Babu,[a,b] Ahmed Kamal [a,c]*

[a]*Medicinal Chemistry and Biotechnology, CSIR-Indian Institute of Chemical Technology, Hyderabad 500007, India*

[b]*Department of Chemistry, Osmania University, Hyderabad 500007, Telangana, India*

[c]*School of Pharmaceutical Education and Research (SPER), Jamia Hamdard, 110 062, New Delhi, India*

Abstract

A library of 1-benzyl-*N*-(2-(phenylamino)pyridin-3-yl)-1*H*-1,2,3-triazole-4-carboxamides (**7a–al**) have been designed, synthesized and screened for their anti-proliferative activity against some selected human cancer cell lines namely DU-145, A-549, MCF-7 and HeLa. Most of them have shown promising cytotoxicity against lung cancer cell line (A549), amongst them **7f** was found to be the most potent anti-proliferative congener. Furthermore, **7f** exhibited comparable tubulin polymerization inhibition (IC_{50} value **2.04**μM) to the standard E7010 (IC_{50} value **2.15**μM). Moreover, flow cytometric analysis revealed that this compound induced apoptosis via cell cycle arrest at G_2/M phase in A549 cells. Induction of apoptosis was further observed by examining the mitochondrial membrane potential and was also confirmed by Hoechst staining as well as Annexin V-FITC assays. Furthermore, molecular docking studies indicated that compound **7f** binds to the colchicine binding site of the β-tubulin. Thus, **7f** exhibits anti-proliferative properties by inhibiting the tubulin polymerization through the binding at the colchicine active site and by induction of apoptosis.

Keywords: 2-anilino-3-aminopyridines, triazole-4-carboxilic acids, apoptosis, cell cycle, colchicine binding, molecular docking and tubulin polymerization.

Corresponding authors Tel: +91-40-27193157; fax: +91-40-27193189, e-mail: ahmedkamal@iict.res.in (A. Kamal)

1. Introduction

Microtubules are cytoskeleton part of the cell residing always in dynamic assemblies of α-tubulin and β-tubulin heterodimers [1–3]. They play a pivotal role during eukaryotic cellular processes such as mitosis, cellular transportation, motility and segregation of chromosomes [4, 5]. The self-assembles of heterodimers form mitotic spindles in dynamic equilibrium, further division of mitotic spindle at the metaphase/anaphase leads to the formation of daughter cells [6]. At this stage, tubulin binding agents (TBAs) disturbs the dynamic equilibrium by stabilizing or destabilizing tubulin polymerization, which leads to apoptotic cell death [7, 8].

During the last few decades, natural products have received much attention as tubulin modulators. Among these, taxanes (paclitaxel, docetaxel) are tubulin polymerization stabilizers/ tubulin polymerization promoters, vinca alkaloids (vinfluine, vinorelbine, vincristine, dolastatins, halichondrins, hemiasterlins and cryptophysin) and colchicines [colchicine (**1**), 2-methoxy estradiol, combretastatin] are tubulin polymerization destabilizers and inhibitors [9–11]. Most of the naturally occurring molecules have certain limitations with respect to their synthesis, solubility, toxicity and resistance [12]. Therefore their derived synthetic molecules have gathered immense acknowledgments across the world with less complexity in their structure, improved solubility with similar biological properties. Combretastatin A-4 (CA-4), **2a** is the simplest naturally occurring tubulin polymerization inhibitor, owing to its limitations, its derived soluble phosphate prodrug CA-4P (**2b**, phosbretabulin or fosbretabulin) emerged as clinical candidate in combination with bevacizumab [13–15].

In recent years, antitumour agents are classified as tubulin-binding tumour vascular disturbing agents (VDAs), they preferentially damage the blood vessels (tissues) of the tumour rather than normal tissues thereby leading to apoptotic cell death [16,17]. The mechanism of tumor vascular disturbing agents is still uncertain however it shows some common characteristics of tubulin polymerization inhibition and binding to the colchicine site of the tubulin [18, 19].
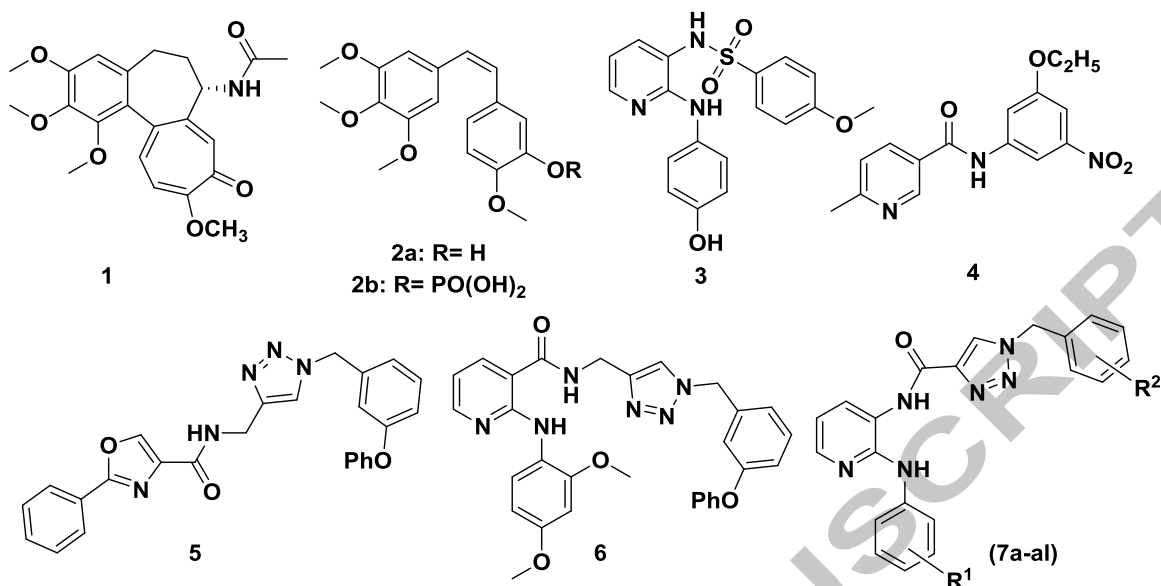
Figure 1: Structures of synthetic and naturally occurring anticancer agents.

E7010 (**3**, **Fig. 1**) is a synthetic pyridine-sulfonamide derivative, that exhibits cytotoxic activity by inhibiting tubulin polymerization [20]. It causes cell cycle arrest by promoting dynamic instability at interphase and binds at β-tubulin colchicine site which leads to apoptosis *via* cell cycle arrest at G_2/M phase [21]. Structure-activity relationship (SAR) studies for E7010 indicate that the pyridine ring system with 2-anilino and 3-sulfonamido substitution improves the solubility and toxicity [22]. Moreover, recent studies have shown that at 3rd position of pyridine with sulfonamide, carbonyl and other functional groups including either open or cyclic partners linking with 4th positions of pyridine (5 and 6 membered heterocyclic ring) are crucial for their cytotoxic activity [23]. Several modifications to the E7010 scaffold have been carried out by omitting the sulfonamide moiety to minimize its toxicity profile. However, E7010 is the only molecule that binds at the three binding zones [24, 25]. Another molecule, *N*-phenyl nicotinamide derivative (**4**) induces apoptosis through cell cycle arrest in G_2/M phase as that of E7010 [26].

Disubstituted 1,2,3-triazole/1,2,4-triazole derivatives possess several biological properties such as histone deacetylase, HSP90 C-terminal and kinase inhibition, inhibition of tubulin polymerization as well as antibacterial activity [27–33]. Most of the biologically active derivatives were prepared by molecular hybridization through the incorporation of 1,2,3-triazole/1,2,4-triazole moiety between 4 or 5 membered heterocyclic ring systems to improve their potency. In addition, *N*-((1-benzyl-1*H*-1,2,3-triazol-4-yl)methyl)nicotinamide (**5**) is one of

the substituted triazole-oxazole carboxamide derivative, arrest cells at G_2/M phase and acts as potent tubulin polymerization inhibitor [31]. Moreover, its related triazole-nicotinamide scaffold was previously developed from this laboratory, one of the compound (**6**) in the series exhibited promising cytotoxicity and potent tubulin polymerization inhibition, **Figure 1** [34].

Based on these observations, we have made an attempt to introduce the triazole-linked carboxamide instead of a sulfonamide group in E7010 scaffold with a view to enhance the biological activity and thereby leading to the target compounds (**7a–al, Fig. 2**).

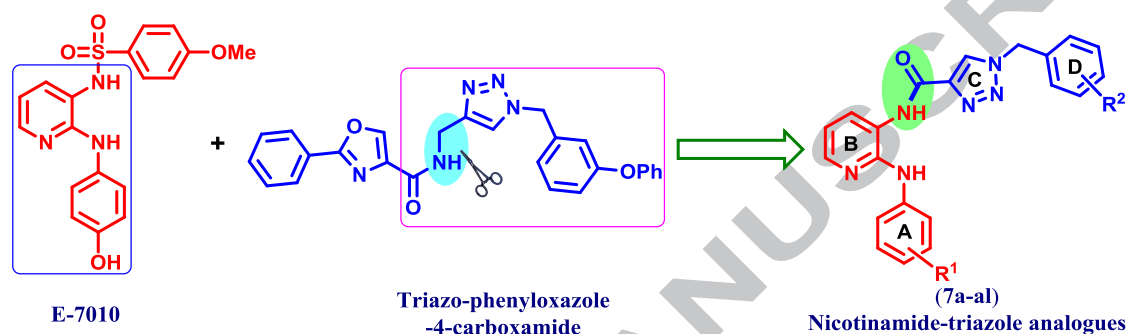**Figure 2:** The design strategy.

2. Results and discussion

2.1. Chemistry

1-Benzyl-*N*-(2-(phenylamino)pyridin-3-yl)-1*H*-1,2,3-triazole-4-carboxamides (**7a–al**) were prepared by acid and amine coupling reaction. The two intermediates, 1-substituted benzyl-1,2,3-triazole-4-carboxilic acids (**15a–f**) and 2-substituted anilinoanilines (**10a–i**) were prepered from the conventional procedures for the synthesis of desired products. One of the intermediates, 1-substituted benzyl-1,2,3-triazole-4-carboxilic acids (**15a–f**) were synthesized by employing different substituted benzyl alcohols (**11a–f**) as a starting material and then reaction with phosphorus tribromide at 0 °C produces substituted benzyl bromides (**12a–f**) [35]. Its corresponding substituted benzyl azides (**13a–f**) were obtained by the reaction with NaN_3 in anhydrous DMSO [36]. The aromatic substituted 1,2,3-triazole methyl ester derivatives (**14a–f**) were obtained by the click reaction with methylpropiolate and substituted benzyl azides (**13a–f**) in the presence of Na-ascorbate, $CuSO_4.5H_2O$ as catalyst in H_2O/t-BuOH (1:2) solvent for 24 h [37]. Finally aromatic substituted 1,2,3-triazole carboxylic acid derivatives (**15a−f**) were obtained through base hydrolysis with 5N NaOH from its corresponding substituted 1,2,3-triazole methyl ester derivatives (**14a–f**) in good to excellent yields (**Scheme 1**).

Scheme 1: Synthetic pathway for the preparation of 1-benzyl-*N*-(2-(phenylamino)pyridin-3-yl)-1*H*-1,2,3-triazole-4-carboxamides.
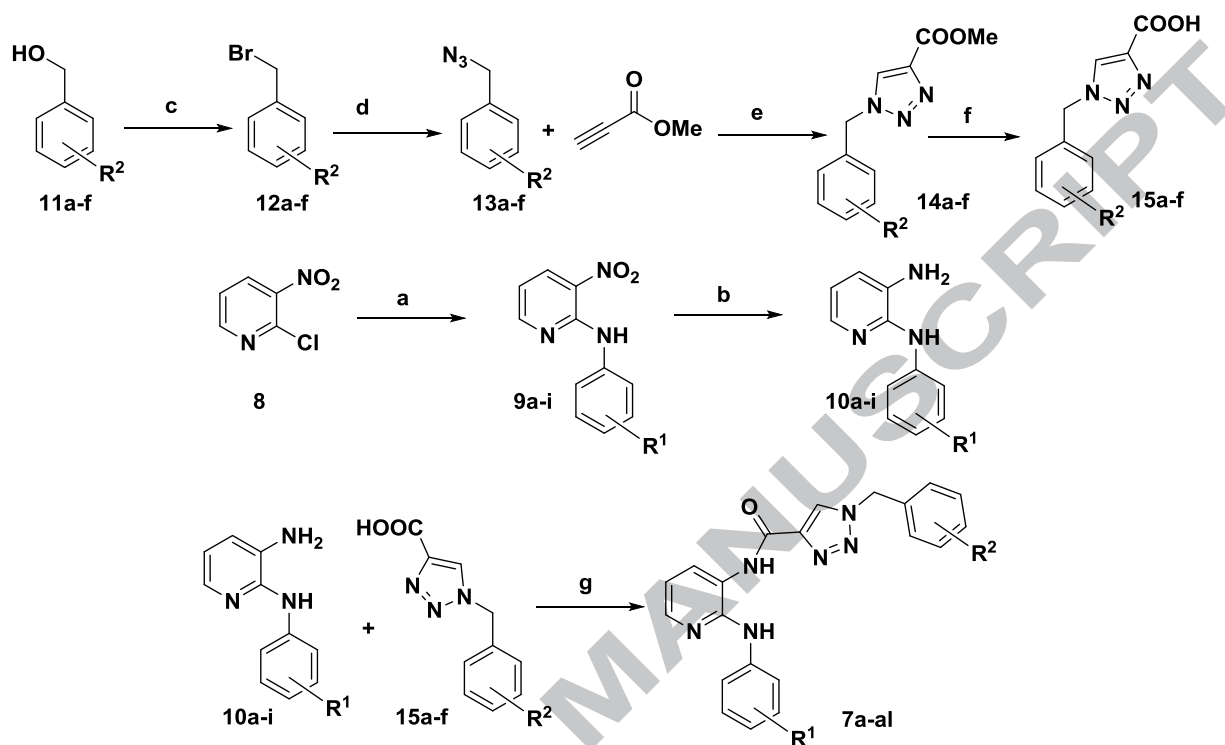
7a: R^1=4-OMe, R^2=3-OPh

7b: R^1=4-OMe, R^2=3-OMe

7c: R^1=4-OMe, R^2=4-OMe

7d: R^1=4-OMe, R^2=4-F

7e: R^1=4-OMe, R^2=3,4,5-triOMe

7f: R^1=3,5-diOMe, R^2=3-OPh

7g: R^1=3,5-diOMe, R^2=3-OMe

7h: R^1=2,4-diOMe, R^2=3-OPh

7i: R^1=2,4-diOMe, R^2=3,4,5-triOMe

7j: R^1=2,4-diOMe, R^2=3-OMe

7k: R^1=2,4-diOMe, R^2=4-OMe

7l: R^1=2,4-diOMe, R^2=4-F

7m: R^1=3,4-diOMe, R^2=3-OPh

7n: R^1=3,4-diOMe, R^2=3-OMe

7o: R^1=3,4,5-triOMe, R^2=3-OPh,

7p: R^1=3,4,5-triOMe, R^2=3,4,5-triOMe

7q: R^1=3,4,5-triOMe, R^2=4-OMe

7r: R^1=3,4,5-triOMe, R^2=3-OMe

7s: R^1=3,4,5-triOMe, R^2=4-F

7t: R^1=H, R^2=3-OPh

7u: R^1=H, R^2=3,4,5-triOMe

7v: R^1=H, R^2=3-OMe

7w: R^1=H, R^2=4-OMe

7x: R^1=H, R^2=4-F

7y: R^1=4-F, R^2=3-OPh

7z: R^1=4-F, R^2=3,4,5-triOMe

7aa: R^1=4-F, R^2=4-OMe

7ab: R^1=4-F, R^2=4-F

7ac: R^1=4-F, R^2=3-OMe

7ad: R^1=4-OH, R^2=3-OPh

7ae: R^1=4-OH, R^2=3,4,5-triOMe

7af: R^1=4-OH, R^2=3-OMe

7ag: R^1=4-OH, R^2=4-OMe

7ah: R^1=4-OH, R^2=4-F

7ai: R^1=4-F, R^2=4-H

7aj: R^1=3,4,5-triOMe, R^2=4-H

7ak: R^1=4-OMe, R^2=4-H

7al: R^1=3-OMe, R^2=4-H

Reagents and conditions: (a) Substituted anilines, ethylene glycol, 160 °C, 6 h, 70-74%; (b) SnCl$_2$·2H$_2$O, EtOH, 60 °C, 6 h, 58-66%; (c) PBr$_3$, ether, 0 °C; (d) NaN$_3$, DMSO, rt, 55-98%; (e) Na Ascorbate (10 mol %), CuSO$_4$·5H$_2$O (5 mol %), H$_2$O/t-BuOH (1:2), rt, 55-98%; (f) 5N NaOH, EtOH, 70°C, 55-98%; (g) EDCI, HOBt, DMF, rt, 73-86%.

Other intermediates 2-anilino-3-aminopyridine derivatives (**10a–i**) were synthesized using 2-chloro-3-nitropyridine (**1**) as starting material, upon reaction with substituted anilines in ethylene glycol at 160 °C to produce substituted 2-anilino-3-nitropyridine derivatives (**9a–i**) [38]. Further, these 2-anilino-3-nitropyridine derivatives (**9a–i**) were subjected to the reduction with $SnCl_2.5H_2O$ to furnish the corresponding substituted 2-anilino-3-aminopyridines (**10a–i**) in good yield. The structure of all these intermediates like anilinoanilines (**10a–i**) and triazolic acids (**15a–f**) were confirmed from their respective ^1H and ^{13}C NMR spectral data that was corroborated with the literature data and was found in accordance [39, 40]. The final amide coupling reaction between substituted acids (**15a–f**) and amines (**10a–i)** was carried out using EDCI/ HOBt and DMAP in DMF solvent at room temperature to obtain the desired substituted-1-benzyl-*N*-(2-(phenylamino)pyridin-3-yl)-1*H*-1,2,3-triazole-4-carboxamide derivatives (**7a–al**) in good yield. Structure of all the target compounds was established on the basis of their ^1H, ^{13}C and HRMS spectral data (**Scheme 1**).

2.2. Biology

2.2.1. Cytotoxicity

To access the cell viability, MTT assay was performed on all the synthesized compounds against four human cancer cell lines viz DU-145 (prostate), A549 (lung), MCF-7 (breast) and HeLa (cervical). E7010 was employed as a standard (positive control) and the results are summarized in **Table 1**. It is observed that these conjugates (**7a–al**) show promising cytotoxicity with IC_{50} values ranging from 1.02 to 42.15 μM against all the cell lines. Notably, compound **7f** was found to be the most active amongst the series with IC_{50} value of **1.02** μM against A549 cells.

Table 1: Cytotoxicity of target compounds (**7a–al**) against selected human cancer cell lines (IC_{50} values in μM).[a]

Compounds codes	DU-145[b]	A549[c]	MCF-7[d]	HeLa[e]
7a	**1.479**	**1.318**	6.462	**1.409**
7b	**1.455**	**1.368**	9.00	9.278
7c	1.738	**1.148**	9.143	8.760
7d	14.78	12.25	21.33	17.05
7e	2.443	2.028	8.030	4.325

7f	**1.549**	**1.023**	2.138	**1.337**
7g	2.884	1.811	8.767	2.291
7h	2.642	**1.435**	7.893	2.938
7i	15.22	7.50	10.66	10.81
7j	3.802	**1.560**	8.455	9.054
7k	9.750	5.115	16.67	12.11
7l	18.25	14.86	33.86	16.21
7m	**1.514**	**1.122**	6.276	6.724
7n	2.051	**1.318**	8.531	6.857
7o	2.410	1.950	14.33	13.30
7p	2.399	1.862	6.857	2.510
7q	3.090	2.109	17.62	8.972
7r	3.548	2.754	15.79	10.47
7s	25.47	18.64	30.43	19.94
7t	14.21	9.143	17.48	16.16
7u	15.71	13.48	18.12	19.89
7v	5.623	7.923	5.623	10.36
7w	6.457	6.273	13.70	4.677
7x	20.42	21.94	23.74	21.81
7y	15.28	10.41	31.12	12.34
7z	17.08	12.93	18.61	21.53
7aa	19.61	9.893	20.20	39.81
7ab	14.29	9.036	23.88	20.06
7ac	10.00	10.62	19.14	24.19
7ad	4.074	3.920	11.59	12.47
7ae	11.99	8.654	17.49	11.96
7af	10.95	5.495	21.82	10.28
7ag	15.26	14.52	24.80	15.96
7ah	26.95	23.61	38.23	27.29
7ai	18.83	14.47	22.65	16.74
7aj	16.32	10.93	17.77	13.09
7ak	20.65	19.12	42.15	11.71
7al	19.10	13.35	32.64	26.29
E7010	1.714	1.622	1.230	2.188

[a]50% Inhibitory concentration after 48h of compounds treatment. [b]Human prostate cancer. [c]Human lung cancer. [d]Human breast cancer. [e]Human cervical cancer.

The structure activity relationship (SAR) of these 1-benzyl-*N*-(2-(phenylamino)pyridin-3-yl)-1*H*-1,2,3-triazole-4-carboxamide derivatives (**7a–7al**) has been studied. The synthesized compounds consist of A, B, C and D ring systems and for all the compounds ring B and C are kept common and the SAR was studied by varying the substitution pattern on ring A as well as ring D. Various analogues have been prepared by placing electron withdrawing and electron donating groups such as 4–F, 4–OH, 4–OMe, 2,4–diOMe, 3,4–diOMe, 3,5–diOMe, 3,4,5–triOMe on ring A. Similarly, 4–F, 3–OMe, 3–OPh, 4–OMe and 3,4,5–triOMe groups incorporated on ring D. In case of the congeners having donating substituents on both the rings (A and D) cytotoxicity values were pronounced. However, the compounds having halogen group (4–F) on D ring are comparably less active (**7d**, **7l, 7s, 7x, 7ab** and **7ah**). Furthermore, the conjugates **7a**, **7f**, **7h**, **7m** and **7o** containing 3–OPh group on D ring and donating groups on A ring have shown significant cytotoxic activity with IC_{50} values ranging from 1.023–14.33 against all the selected cancer cell lines. Amongst them, compound **7f** that contains 3,5–diOMe group on ring A and 3–OPh group on ring D was found to be the most potent hybrid. Replacing the substitution pattern on A ring from 3,5–diOMe to 3,4–diOMe and 4–OMe without changing the substitution pattern on D ring (3–OPh) reduces the in cytotoxic activity (**7m** and **7a**). Moreover, when 3, 4 and 5 positions of ring A masked by methoxy group without changing the substitution pattern of ring D (3–OPh), drastic fall in the cytotoxic activity has observed (**7o**). Furthermore, removal of all the substituents or placing hydroxy group or electron withdrawing halogen such as F on ring A without changing the substitution pattern on ring D i.e., 3–OPh progressively decreases the cytotoxicity (**7t**, **7y**, and **7ad**). Finally, based on the above results it can be summarized that cytotoxic activity order for the presence of donating and withdrawing groups on A ring with same substitution on D ring is as follows; 3,5–diOMe > 3,4–diOMe > 4–OMe ~ 2,4–diOMe > 3,4,5–triOMe > 4–H > 4–OH > 4–F.

Replacing the 3–OPh group on D ring with substitutions like 3–OMe, 4–OMe, 3,4,5–triOMe, 4–F and without changing the substitution pattern on ring A (2,4–diOMe) exhibited 2–8 fold reduction in cytotoxicity (**7h** > **7j** > **7k** > **7i** > **7l**). Similarly, reduction in cytotoxicity can be compared equally between substitutions on A ring with that of D ring (decreasing order of cytotoxicity **7a–7e**, **7h–7l**, **7o–7s, 7t–7x**, **7y–7ac**, **7ad–7ah** and **7ai–7al**). Based on these observations, the effect of changing the substituents on D ring in relation to constant substituent on A ring, it is observed that the cytotoxicity decreasing in the following

order 3–OPh> 3–OMe > 4–OMe > 3,4,5–triOMe > 4–H (**Fig. 3**). Most of the synthesized compounds have shown relatively improved cytotoxicity against A-549 cell line. Interestingly, compounds with donating groups on both the A and D ring systems exhibit better activity than the reference standard E7010 (**7a**, **7b**, **7c**, **7f**, **7h**, **7m** and **7n).** Therefore, it can be concluded that electron donating groups on both the rings are necessary for prominent cytotoxic activity. Hence detailed studies were carried out on one of the potent representative compound **7f**.
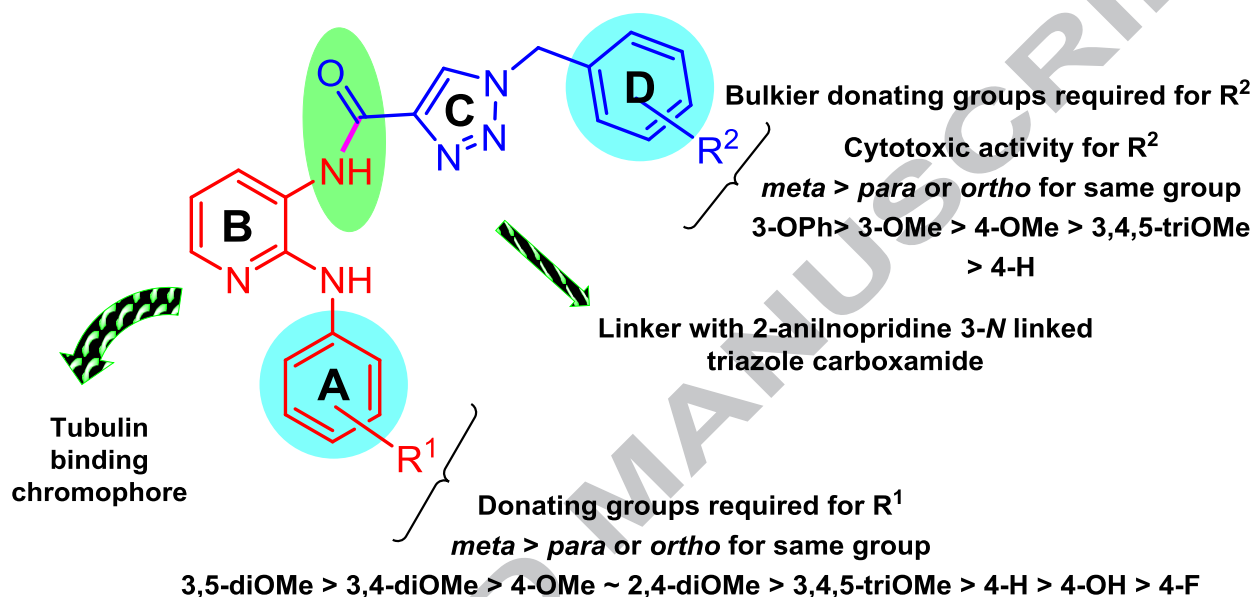

Figure 3: Structure–activity relationship for the 1-benzyl-*N*-(2-(phenylamino)pyridin-3-yl)-1*H*-1,2,3-triazole-4-carboxamide derivatives (**7a**–**al**)

2.2.2. Cell cycle analysis

Many anticancer compounds exert their growth inhibitory effect either by arresting the cell cycle at a particular checkpoint of cell cycle or by induction of apoptosis or a combination of both [41]. The screening results revealed that compound **7f** showed significant anticancer activity against human lung cancer cell line (A549). Further, we performed a cell cycle analysis to confirm whether the cell growth inhibition of human lung cancer cells was due to cell cycle arrest. In this study, A549 cells were treated with the compound **7f** for 48 h at 1 and 2 μM concentrations and it indicates that **7f** has shown G_2/M cell cycle arrest in comparison with the control cells. Compound **7f** displayed 60.79 % of cell accumulation in G_2/M phase at 1 μM

concentration, whereas it exhibited 77.31 % of cell accumulation at 2 µM concentration (**Fig. 4** and **Table 2**).
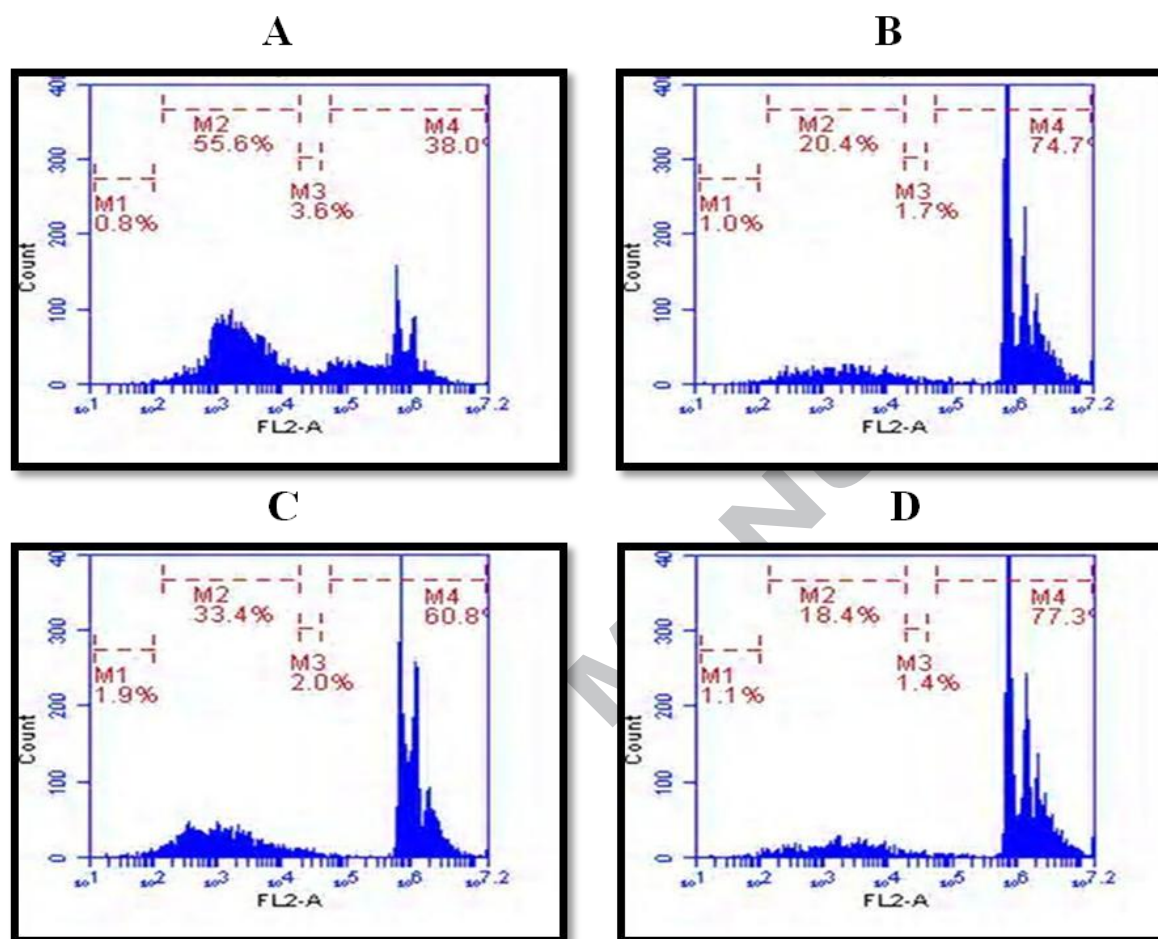

Figure 4: Flow cytometric analysis in A549 cells after treatment with compound **7f** at 1 and 2 µM concentrations for 48 h. A: Control cells (A549), B: E7010 (2 µM), C: **7f** (1 µM) and D: **7f** (2 µM).

Table 2: Effect of compound **7f** on cell cycle phase distribution in A549 cells

Sample	Sub G_1 %	G_0/G_1 %	S %	G_2/M %
A: Control cells	0.81	55.60	3.64	38.04
B: E7010 (2 µM)	0.99	20.41	1.72	74.73
C: **7f** (1 µM)	1.92	33.38	1.96	60.79

D: **7f** (2 μM)	1.05	18.41	1.43	77.31

2.2.3. Effect of compounds on tubulin polymerization

In general G_2/M cell cycle arrest is associated with inhibition of tubulin polymerization and since compound **7f** causes cell cycle arrest at G_2/M cell cycle arrest; thus its effect on microtubule inhibitory function was also investigated. Tubulin subunits are known to heterodimerize and self-assemble to form microtubules in a time dependent manner. Thus, the progression of tubulin polymerization [42–45] was examined by monitoring the increase in fluorescence emission at 420 nm (excitation wavelength is 360 nm) in 384 well plate for 1 h at 37 °C with and without the compound at 3 μM concentration in comparison with reference compound E7010. Compound **7f** significantly inhibited tubulin polymerization by 64.77 %, which is comparable with E7010 (**Fig. 5**). This was followed by the evaluation of IC_{50} value for compound **7f** and the experimental results revealed that this compound shows 2.04 μM IC_{50} value suggesting that it inhibits the tubulin polymerization.
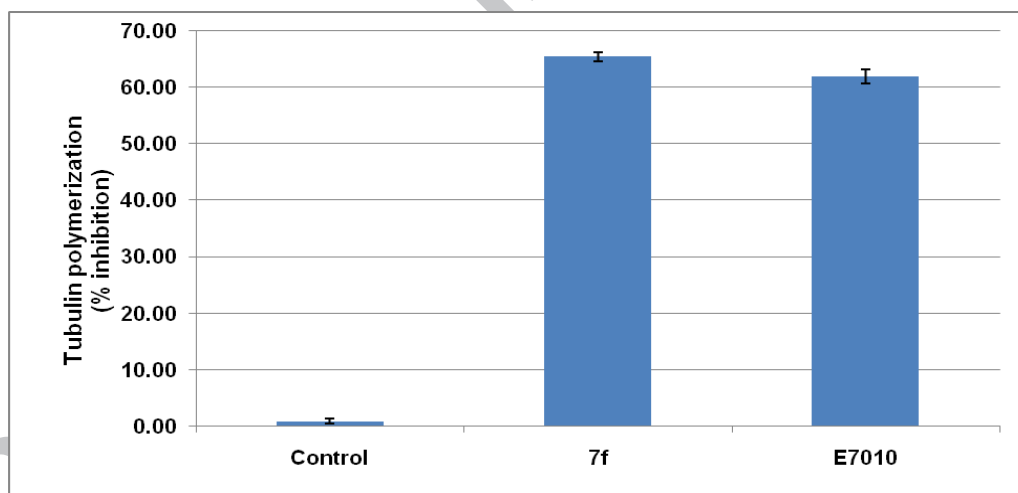

Figure 5: Effect of compound **7f** on tubulin polymerization: tubulin polymerization was monitored by the increase in fluorescence at 360 nm (excitation) and 420 nM (emission) for 1 h at 37 °C. E7010 was used as the reference compound in this study. Values indicated are the mean ± SD of two different experiments.

2.2.4. Hoechst staining assay

Apoptosis, with its classic characteristics of chromatin condensation and fragmented nuclei is one of the major pathways that lead to the process of cell death [46]. The apoptosis inducing capability of this potent compound was studied by Hoechst staining method. In this study, A549 cells were treated with **7f** at 1 and 2 µM concentrations for 48 h. From these results, it can be inferred that this compound induced apoptotic cell death in human lung cancer cells A549 (**Fig. 6**).
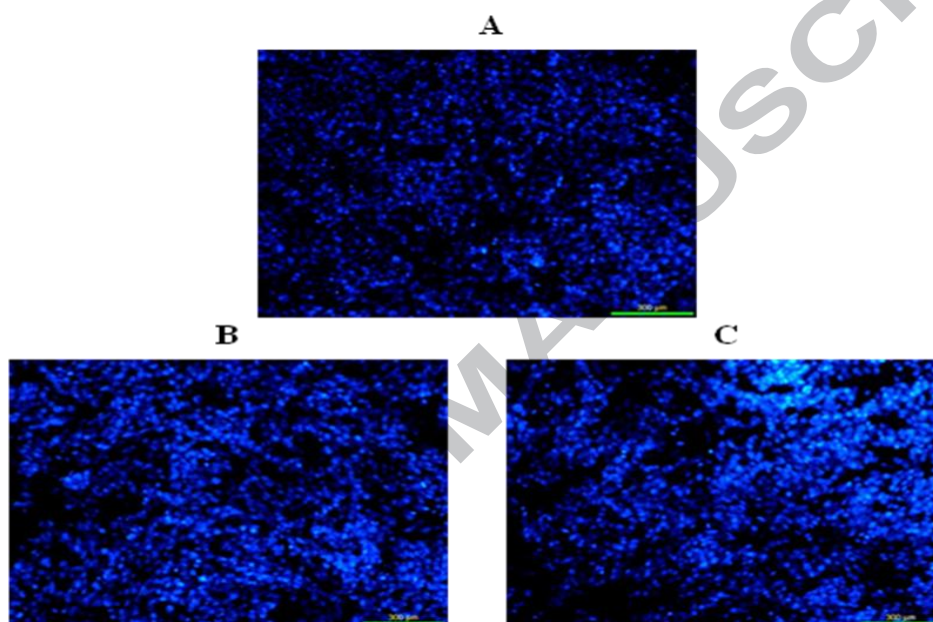

Figure 6: Hoechst staining in A549 cell line; A: Control cells, B: **7f** (1 µM) and **7f** (2 µM).

2.2.5. Measurement of mitochondrial membrane potential (ΔΨm)

The maintenance of mitochondrial membrane potential (ΔΨm) is important for the mitochondrial integrity and bioenergetic function [47]. Mitochondrial changes, including loss of mitochondrial membrane potential ((ΔΨm) are key events that take place during drug induced apoptosis. In order to study the apoptosis inducing effect of compound **7f**, mitochondrial membrane potential ((ΔΨm) changes were detected using the fluorescent probe JC 1 (5,5,6,6-tetrachloro-1,1,3,3-tetraethylbenzimidazolocarbocyanine iodide-5 mg/mL). After 48 h of the treatment by the compound, it was observed that the mitochondrial membrane potential (ΔΨm) of A549 cells reduced significantly (**Fig. 7**).
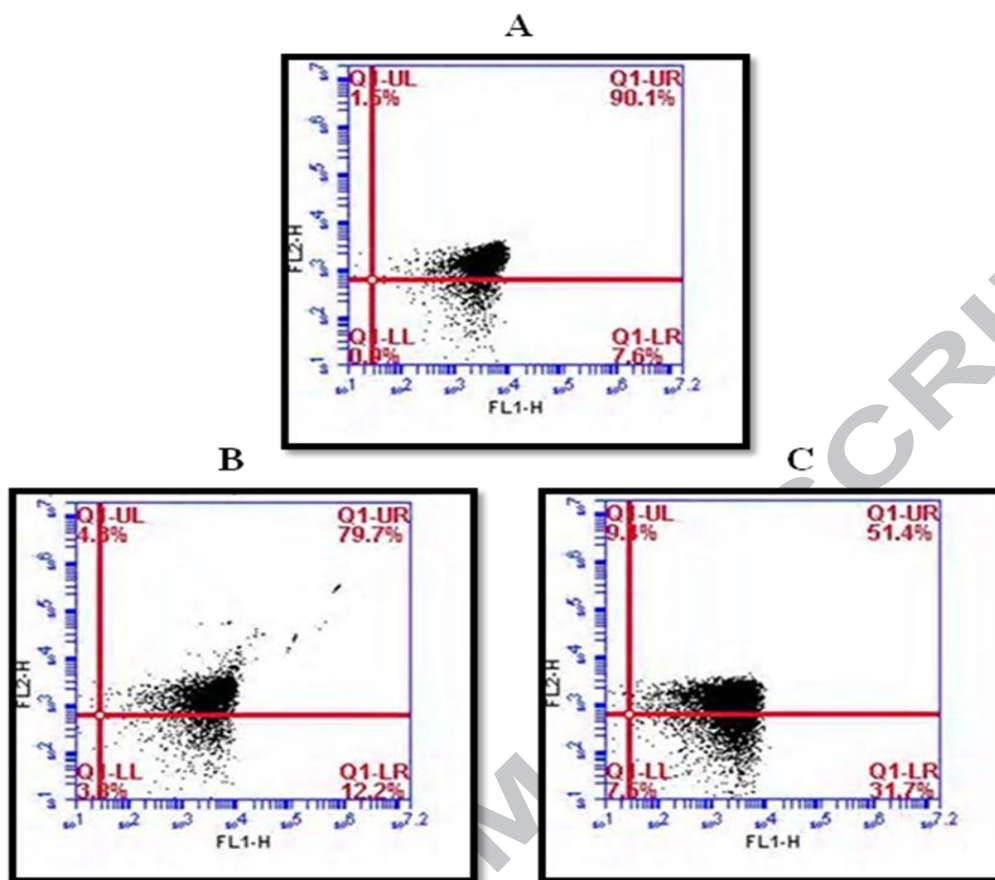
Figure 7: Effect of compound **7f** on mitochondrial membrane potential (($\Delta\Psi$m): Drops in membrane potential ($\Delta\Psi$m) was assessed by JC-1 staining of A549 cells treated with test compound and samples were then subjected to flow-cytometry analysis on a FACS (Becton Dickinson) in the FL1, FL2 channel to detect mitochondrial potential. A: Control cells, B: **7f** (1 μM) and C: **7f** (2 μM).

2.2.6. Annexin V-FITC assay

The apoptotic effect of **7f** was further evaluated by Annexin V FITC/PI (AV/PI) dual staining assay [48] to examine the occurrence of phosphatidylserine externalization and also to understand whether it is due to physiological apoptosis or nonspecific necrosis. In this study, A549 cells were treated with this compound for 48 h at 1 and 2 μM concentrations to examine the apoptotic effect. It was observed that this compound showed significant apoptosis against A549 cells as shown in **Fig. 4**. These results indicated that compound **7f** has shown 19.26 and 34.86 % at 1 and 2 μM concentrations respectively (**Fig. 8** and **Table 3**).
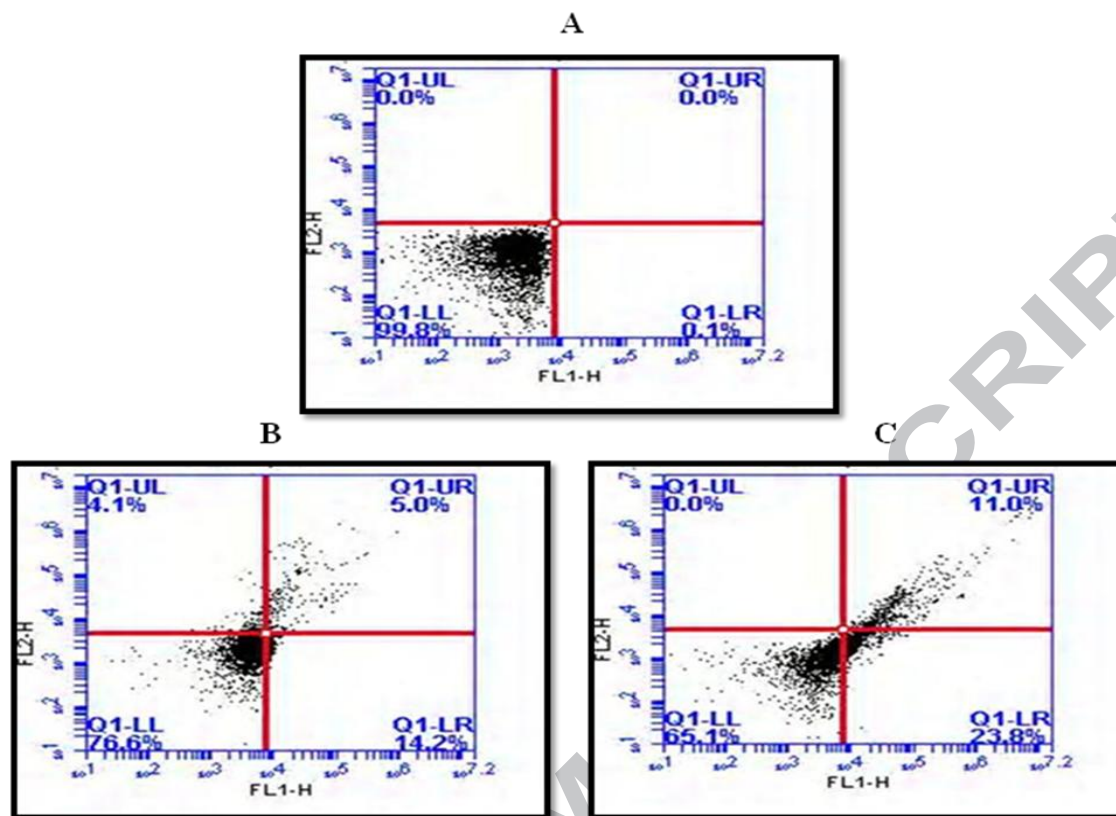
Figure 8: Annexin V-FITC staining. A: Control cells (A549), B: Nocodazole (2 μM) and C: **7f** (1 μM) and D: **7f** (2 μM).

Table 3: Annexin V-FITC assay.

Sample	UL %	UR %	LL%	LR %
A: Control cells	0.04	0.01	99.84	0.12
C: 7f (1 μM)	4.12	5.01	76.62	14.25
D: 7f (2 μM)	0.01	11.02	65.14	23.84

2.3. Molecular docking studies

Molecular docking is a vital component in bioinformatics to exploit the structure of protein–small molecule complexes in structural detail, which plays a pivotal role in drug discovery and development. Docking is an algorithm, which predicts the preferred relative orientation of one molecule (ligand) when bound in an active site of another molecule (protein) to form a stable complex such that free energy of the overall system is minimized. Docking

involves two consecutive steps, initially sampling conformations of the ligand in the binding pocket of the protein and followed by ranking these conformations via a scoring function.

Cytotoxic results of these conjugates (especially compounds like **7a, 7b, 7c, 7f, 7g, 7h, 7j, 7m** and **7n** on human lung cancer cell lines) encouraged us to perform their molecular docking studies. Here, molecular docking tool was used to predict the 3D complex of the 1-benzyl-*N*-(2-(phenylamino)pyridin-3-yl)-1*H*-1,2,3-triazole-4-carboxamides conjugates within the constraints of E7010 binding pocket present in the tubulin (PDB ID: 3HKC) [49]. The co-ordinates of the crystal structure were obtained from RCSB-Protein Data Bank and suitable corrections to it were made by using Protein Preparation Wizard from Schrödinger package. In regard to the ligands, molecules were constructed using ChemBio3D Ultra 12.0 and their geometries were optimized using molecular mechanics. Finally, docking studies were performed for the most active conjugate **7f** and reference ligand **E7010** by using Auto Dock 4.2 [50] and the results were visualized through PyMOL [51].
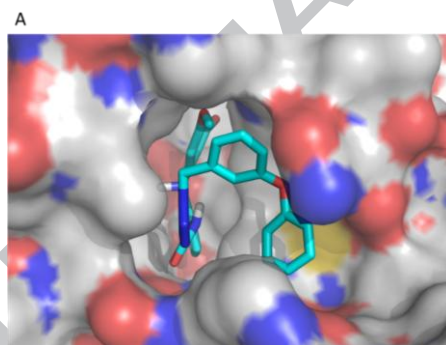

Figure 9: Surface binding pose of compound **7f** in E7010 binding pocket present in β-subunit of tubulin, where the protein is shown as a surface representation.

Docking studies revealed that conjugate **7f** fit well in the colchicine binding site present in β-subunit at α-β interface of the tubulin (**Fig. 9**). In addition, free binding energies for compound **7f** and E7010 were found to be -13.00 and -9.15 respectively. In spite of having structural similarities with co-crystal ligand (E7010), conjugate **7f** exhibited unique binding poses (**Fig. 10A**). 1-(3-Phenoxybenzyl)-1*H*-1,2,3-triazole-4-carboxylic acid and methoxybenzene sulfonamide moieties present in conjugate **7f** and E7010 respectively protrude towards the α-subunit, N^2-substituted phenylpyridine-2,3-diamine motifs present in both the ligands precisely fit into the β-subunit, pyridine-2,3-diamine ring present in the conjugate **7f** is deeply embedded

in to the β-subunit compared to same ring present in E7010. Methoxy oxygen present in conjugate **7f** shows hydrogen bonding with amide protons of Leu252 amino acid residue of β-subunit (red dash lines in **Fig. 10B**) and bond length is recorded as 2.64 Å. Further, conjugate **7f** showed several hydrophobic interactions with the side chain of Gln136, Asn167, Phe169, Tyr202, Val238, Cys241, Leu242, Leu248, Leu255, Asn258, Met259, Lys352, Thr376, Ile378 amino acid residues of β-subunit and Asn101, Val181 residues present in α-subunit. In addition, the same conjugate showed interactions with peptide backbones of Gly237, Val238, Thr239, Ala250, Asn251, Leu252, Leu254, Leu255, Thr314, Val315, Ala316, Ala317, Val318, Asn350, Val351, Lys352, Thr353, Ala354, Thr376, Phe377 and Ile378 residues present in the β-subunit (**Fig. 10B**).
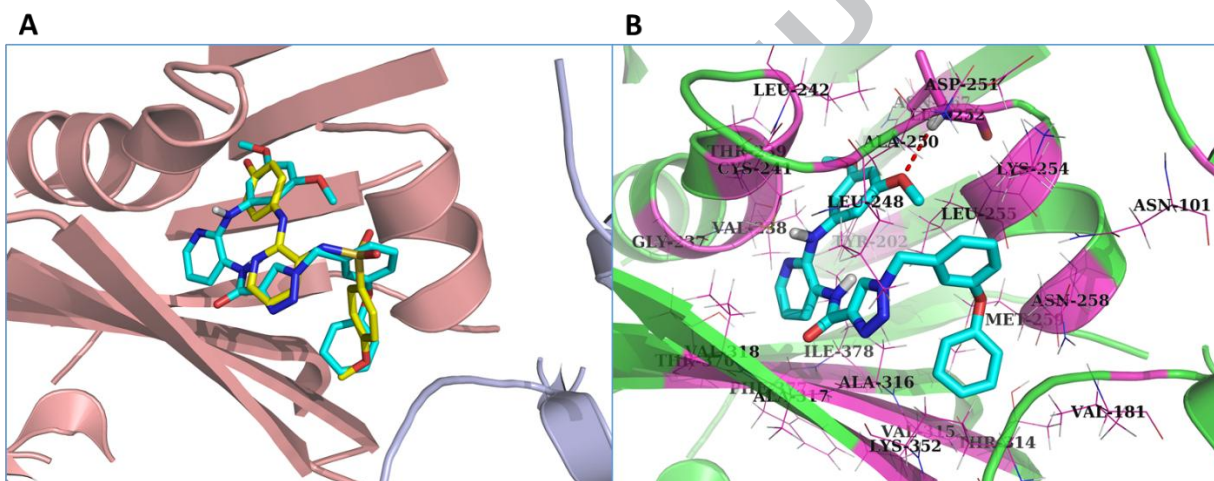

Figure 10: A) Binding pose comparison of conjugate **7f** with co-crystal ligand (E70), **B**) Binding pose of conjugate **7f**, including hydrogen bonding and hydrophobic interactions in colchicine binding pocket of tubulin where protein is shown as a cartoon representation. Conjugate **7f** and E7010 were shown in stick and coloured by the atom type. Carbon: cyan, yellow; oxygen: red; hydrogen: white; nitrogen: blue; sulphur.

3. Conclusion

A series of substituted-1-benzyl-*N*-(2-(phenylamino)pyridin-3-yl)-1*H*-1,2,3-triazole-4-carboxamides (**7a–al**) were designed, synthesized and evaluated for their cytotoxic activity against DU-145, A-549, MCF-7 and HeLa human cancer cell lines. Most of the compounds have shown moderate to promising cytotoxicity. Interestingly, compounds with donating groups have shown profound cytotoxic activity against A549 cell line. Among these, compound **7f** was found

to be the most active congener against human lung cancer cells with IC$_{50}$ value of **1.023** µM. Interestingly, the cell cycle analysis has shown that these derivatives arrested the cells in G$_2$/M phase and also inhibited microtubule assembly effectively in comparison to standard E7010. Moreover, Hoechst staining, mitochondrial membrane potential (ΔΨm) and Annexin V-FITC assays in human lung cancer cells confirmed the induction of apoptosis. In addition, the molecular docking studies revealed that **7f** interacted efficiently with the tubulin protein *via* binding at the E7010 binding site of the tubulin. On the basis of all these studies, it can be concluded that conjugate **7f** showed promising cytotoxicity by inhibiting tubulin polymerization. This compound (**7f**) could be further explored in detail and has a potential to be considered as a lead from this type of a scaffold.

4. Experimental Protocols

4.1. Materials and methods

All Chemicals and reagents were purchased from the commercial suppliers Alfa Aesar, Sigma Aldrich and used without further purification. The reaction progress was monitored by Thin layer chromatography (TLC) was performed using pre-coated silica gel 60 F$_{254}$ MERCK. TLC plates were visualized and analyzed by exposure to UV light or iodine vapors and aqueous solution of ninhydrin. Column chromatography was performed with Merck flash silica gel with 60–120 mesh size. Melting points were determined on an Electro thermal melting point apparatus and are uncorrected. Nuclear magnetic resonance spectra for ^{1}H NMR was obtained on Avance 300, 400 and 500 MHz and analyzed using MestReNova software and the chemical shifts are reported in ppm from tetramethylsilane(0 ppm) or the solvent resonance as the internal standard (CDCl$_3$ 7.26 ppm, DMSO-d_6 2.49 ppm) and for ^{13}C NMR the chemical shifts are reported in ppm from the solvent resonance as the internal standard (CDCl$_3$ 77ppm, DMSO-d_6 39.3ppm). HRMS was performed on a Varian ESI- QTOF instrument.

4.2. General synthetic procedure for the preparation of compounds (7a–7al)

To a solution of 1-substituted benzyl-1,2,3-triazole-4-carboxilic acid (**15a–f**, 1 mmol) in dry DMF, EDCI (1.2 mmol) and HOBT (1.2 mmol) were added and the reaction mixture was stirred for 20 min. To the reaction mixture, 2-substituted anilinoaniline (**10a–i**, 1 mmol) was added and further stirred at room temperature for 12 h. The contents of the reaction mixture were

poured into ice-cold water (50 mL), extracted with ethyl acetate (50 mL). The organic layer was washed with 5% HCl (2x20 mL), 5% NaHCO$_3$ (2x20 mL), and brine solution (20 mL). The organic layer was separated, dried over anhydrous Na$_2$SO$_4$, filtered and the solvent was removed to give a crude product which was purified by chromatography (ethyl acetate/hexanes) to give the desired product (**7a–al**).

4.2.1.   N-(2-((4-methoxyphenyl)amino)pyridin-3-yl)-1-(3-phenoxybenzyl)-1H-1,2,3-triazole-4-carboxamide (7a)

Light brown solid, Yield 82%, M.P: 138−140 °C; ^{1}H NMR (500 MHz, CDCl$_3$) δ 8.72 (s, 1H), 8.14 (dd, J_1 = 4.8 Hz, J_2 = 1.6 Hz, 1H), 8.09 (s, 1H), 7.75 (dd, J_1 = 7.7 Hz, J_2 = 1.6 Hz, 1H), 7.40 − 7.33 (m, 3H), 7.29 − 7.27 (m, 2H), 7.16 (t, J = 7.4 Hz, 1H), 7.04 − 6.98 (m, 4H), 6.96 (d, J = 1.9 Hz, 1H), 6.87 − 6.85 (m, 2H), 6.83 (dd, J_1 = 7.7 Hz, J_2 = 4.9 Hz, 1H), 6.69 (s, 1H), 5.56 (s, 2H), 3.78 (s, 3H); ^{13}C NMR (125 MHz, CDCl$_3$) δ 158.92, 158.36, 156.27, 155.49, 150.71, 145.85, 143.01, 135.37, 133.69, 133.04, 130.76, 130.00, 126.00, 124.05, 122.63, 122.54, 119.42, 119.31, 118.91, 118.25, 115.20, 114.29, 55.54, 54.35; MS (ESI): *m/z* 493 [M+H]$^+$; HRMS (ESI) Calcd for C$_{29}$H$_{26}$N$_5$O$_3$ [M+H]$^+$ 493.1983; Found: 493.1999.

4.2.2.   1-(3-Methoxybenzyl)-N-(2-((4-methoxyphenyl)amino)pyridin-3-yl)-1H-1,2,3-triazole-4-carboxamide (7b)

White solid, Yield 81%, M.P: 145−147 °C; ^{1}H NMR (300 MHz, CDCl$_3$) δ 8.73 (s, 1H), 8.13 (dd, J_1 = 4.9 Hz, J_2 = 1.6 Hz, 1H), 8.06 (s, 1H), 7.74 (dd, J_1 = 7.7 Hz, J_2 = 1.5 Hz, 1H), 7.33 (t, J = 7.6 Hz, 1H), 7.30 − 7.26 (m, 2H), 6.96 − 6.87 (m, 2H), 6.87 − 6.82 (m, 3H), 6.82 − 6.78 (m, 1H), 6.72 (s, 1H), 5.55 (s, 2H), 3.81 (s, 3H), 3.78 (s, 3H); ^{13}C NMR (125 MHz, CDCl$_3$) δ 160.27, 158.96, 155.47, 150.72, 145.82, 142.96, 134.92, 133.74, 133.03, 130.51, 125.98, 122.51, 120.50, 119.35, 115.19, 114.51, 114.29, 114.17, 55.55, 55.38, 54.65; MS (ESI): *m/z* 431 [M+H]$^+$; HRMS (ESI) Calcd for C$_{29}$H$_{26}$N$_5$O$_3$ [M+H]$^+$ 431.1826; Found: 431.1849.

4.2.3.   1-(4-Methoxybenzyl)-N-(2-((4-methoxyphenyl)amino)pyridin-3-yl)-1H-1,2,3-triazole-4-carboxamide (7c)

White solid, Yield 82%, M.P: 170−172 °C; ^{1}H NMR (500 MHz, CDCl$_3$) δ 8.72 (s, 1H), 8.12 (dd, J_1 = 4.9 Hz, J_2 = 1.6 Hz, 1H), 8.01 (s, 1H), 7.73 (dd, J_1 = 7.7 Hz, J_2 = 1.5 Hz, 1H), 7.27 (d, J =

1.4 Hz, 2H), 7.25 (d, J = 3.5 Hz, 2H), 6.95 – 6.90 (m, 2H), 6.87 – 6.83 (m, 2H), 6.81 (dd, J_1 = 7.7 Hz, J_2 = 4.9 Hz, 1H), 6.73 (s, 1H), 5.51 (s, 2H), 3.82 (s, 3H), 3.77 (s, 3H); ^{13}C NMR (125 MHz, CDCl$_3$) δ 160.31, 159.00, 155.49, 150.71, 145.77, 142.85, 133.73, 133.04, 130.01, 125.73, 125.45, 122.52, 119.38, 115.18, 114.76, 114.30, 55.56, 55.42, 54.30; MS (ESI): m/z 431 [M+H]$^+$; HRMS (ESI) Calcd for C$_{29}$H$_{26}$N$_5$O$_3$ [M+H]$^+$ 431.1826; Found: 431.1847.

4.2.4.   1-(4-Fluorobenzyl)-N-(2-((4-methoxyphenyl)amino)pyridin-3-yl)-1H-1,2,3-triazole-4-carboxamide (7d)

White solid, Yield 83%, M.P: 159−161 °C; ^{1}H NMR (500 MHz, CDCl$_3$) δ 8.73 (s, 1H), 8.13 (dd, J_1 = 4.8 Hz, J_2 = 1.3 Hz, 1H), 8.06 (s, 1H), 7.76 – 7.72 (m, 1H), 7.31 (dd, J_1 = 8.5 Hz, J_2 = 5.2 Hz, 2H), 7.27 (d, J = 4.1 Hz, 2H), 7.10 (dd, J_1 = 14.2 Hz, J_2 = 5.7 Hz, 2H), 6.85 (d, J = 8.9 Hz, 2H), 6.82 (dd, J_1 = 7.7 Hz, J_2 = 4.9 Hz, 1H), 6.71 (s, 1H), 5.56 (s, 2H), 3.78 (s, 3H); ^{13}C NMR (125 MHz, CDCl$_3$) δ 164.10, 162.12, 158.88, 155.50, 150.68, 145.85, 143.06, 133.72, 133.04, 130.31 (d, J_{C-F} = 8.4 Hz), 125.86, 122.49, 119.34, 116.44 (d, J_{C-F} = 21.9 Hz), 115.23, 114.30, 55.55, 53.94; MS (ESI): m/z 419 [M+H]$^+$; HRMS (ESI) Calcd for C$_{29}$H$_{26}$N$_5$O$_3$ [M+H]$^+$ 419.1626; Found: 419.1649.

4.2.5.   N-(2-((4-methoxyphenyl)amino)pyridin-3-yl)-1-(3,4,5-trimethoxybenzyl)-1H-1,2,3-triazole-4-carboxamide (7e)

White solid, Yield 81%, M.P: 172−174 °C; ^{1}H NMR (500 MHz, CDCl$_3$) δ 8.74 (s, 1H), 8.13 (dd, J_1 = 4.8 Hz, J_2 = 1.5 Hz, 1H), 8.08 (s, 1H), 7.75 (dd, J_1 = 7.7 Hz, J_2 = 1.5 Hz, 1H), 7.28 − 7.26 (m, 2H), 6.87 − 6.83 (m, 2H), 6.82 (dd, J_1 = 7.7 Hz, J_2 = 4.9 Hz, 1H), 6.73 (s, 1H), 6.54 (s, 2H), 5.49 (s, 2H), 3.85 (d, J = 1.0 Hz, 9H), 3.77 (s, 3H); ^{13}C NMR (125 MHz, CDCl$_3$) δ 158.96, 155.46, 153.88, 150.66, 145.85, 142.92, 138.65, 133.68, 132.98, 128.87, 125.88, 122.48, 119.33, 115.23, 114.26, 105.61, 60.91, 56.26, 55.53, 55.02; MS (ESI): m/z 491 [M+H]$^+$; HRMS (ESI) Calcd for C$_{29}$H$_{26}$N$_5$O$_3$ [M+H]$^+$ 491.2037; Found: 491.2055.

4.2.6. N-(2-((3,5-dimethoxyphenyl)amino)pyridin-3-yl)-1-(3-phenoxybenzyl)-1H-1,2,3-triazole-4-carboxamide (7f)

Brown solid, Yield 78%, M.P: 121−123 °C; ^{1}H NMR (300 MHz, CDCl$_3$) δ 8.87 (s, 1H), 8.21 − 8.13 (m, 1H), 8.08 (s, 1H), 7.83 (d, J = 6.6 Hz, 1H), 7.35 (q, J = 7.4 Hz, 3H), 7.14 (t, J = 7.4 Hz,

1H), 7.07 – 6.93 (m, 6H), 6.89 (dd, J_1 = 7.7 Hz, J_2 = 4.9 Hz, 1H), 6.56 (d, J = 2.1 Hz, 2H), 6.11 (t, J = 2.0 Hz, 1H), 5.52 (s, 2H), 3.73 (s, 6H); ^{13}C NMR (125 MHz, CDCl$_3$) δ 161.14, 158.95, 158.36, 156.27, 149.35, 145.69, 142.96, 142.73, 135.36, 132.87, 130.76, 129.99, 126.04, 124.04, 122.63, 120.85, 119.42, 118.91, 118.25, 116.47, 97.86, 94.58, 55.31, 54.36; MS (ESI): m/z 523 $[M+H]^+$; HRMS (ESI) Calcd for C$_{29}$H$_{26}$N$_5$O$_3$ $[M+H]^+$ 523.2088; Found: 523.2113.

4.2.7. N-(2-((3,5-dimethoxyphenyl)amino)pyridin-3-yl)-1-(3-methoxybenzyl)-1H-1,2,3-triazole-4-carboxamide (7g)

White solid, Yield 84%, M.P: 152−154 °C; ^{1}H NMR (500 MHz, CDCl$_3$) δ 8.83 (s, 1H), 8.19 (dd, J_1 = 4.8 Hz, J_2 = 1.7 Hz, 1H), 8.07 (s, 1H), 7.83 (dd, J_1 = 7.8 Hz, J_2 = 1.6 Hz, 1H), 7.36 − 7.30 (m, 1H), 6.91 (qd, J = 8.8, 3.3 Hz, 4H), 6.85 − 6.81 (m, 1H), 6.56 (d, J = 2.2 Hz, 2H), 6.12 (t, J = 2.2 Hz, 1H), 5.54 (s, 2H), 3.81 (s, 3H), 3.75 (s, 6H); ^{13}C NMR (75 MHz, CDCl$_3$) δ 161.11, 160.24, 159.00, 149.37, 145.68, 142.88, 142.73, 134.90, 132.92, 130.51, 126.04, 120.82, 120.51, 116.44, 114.51, 114.14, 97.82, 94.53, 55.37, 55.31, 54.65; MS (ESI): m/z 461 $[M+H]^+$; HRMS (ESI) Calcd for C$_{29}$H$_{26}$N$_5$O$_3$ $[M+H]^+$ 461.1932; Found: 461.1948.

4.2.8. N-(2-((2,4-dimethoxyphenyl)amino)pyridin-3-yl)-1-(3-phenoxybenzyl)-1H-1,2,3-triazole-4-carboxamide (7h)

White solid, Yield 84%, M.P: 141−143 °C; ^{1}H NMR (500 MHz, CDCl$_3$) δ 8.72 (s, 1H), 8.13 (dd, J_1 = 4.9 Hz, J_2 = 1.5 Hz, 1H), 8.10 (s, 1H), 7.86 (dd, J_1 = 12.7 Hz, J_2 = 4.9 Hz, 2H), 7.36 (q, J = 7.7 Hz, 3H), 7.15 (t, J = 7.4 Hz, 1H), 7.05 − 6.94 (m, 5H), 6.82 (dd, J_1 = 7.5 Hz, J_2 = 5.1 Hz, 2H), 6.53 − 6.46 (m, 2H), 5.55 (s, 2H), 3.80 (s, 3H), 3.79 (s, 3H); ^{13}C NMR (100 MHz, CDCl$_3$) δ 158.91, 158.37, 156.30, 155.36, 150.33, 150.28, 145.48, 143.25, 135.46, 132.70, 130.76, 130.00, 125.95, 124.05, 123.65, 122.64, 120.53, 119.85, 119.43, 118.92, 118.26, 115.19, 103.94, 99.06, 55.84, 55.63, 54.37; MS (ESI): m/z 523 $[M+H]^+$; HRMS (ESI) Calcd for C$_{29}$H$_{26}$N$_5$O$_3$ $[M+H]^+$ 523.2088; Found: 523.2114.

4.2.9. N-(2-((2,4-dimethoxyphenyl)amino)pyridin-3-yl)-1-(3,4,5-trimethoxybenzyl)-1H-1,2,3-triazole-4-carboxamide (7i)

White solid, Yield 76%, M.P: 184−186°C; ^{1}H NMR (300 MHz, CDCl$_3$) δ 8.73 (s, 1H), 8.13 (dd, J_1 = 5.7 Hz, J_2 = 2.4 Hz, 2H), 7.91 − 7.79 (m, 2H), 6.83 (dd, J_1 = 7.8 Hz, J_2 = 5.0 Hz, 2H), 6.55

(s, 2H), 6.52 – 6.46 (m, 2H), 5.51 (s, 2H), 3.85 (d, J = 1.5 Hz, 9H), 3.81 (s, 3H), 3.79 (s, 3H); ^{13}C NMR (75 MHz, CDCl$_3$) δ 158.94, 155.39, 153.90, 150.35, 150.21, 145.48, 143.17, 132.58, 128.94, 125.98, 125.83, 123.60, 120.60, 119.89, 115.24, 105.62, 103.96, 99.06, 60.92, 56.27, 55.82, 55.61, 55.03; MS (ESI): m/z 521 [M+H]$^+$; HRMS (ESI) Calcd for C$_{29}$H$_{26}$N$_5$O$_3$ [M+H]$^+$ 521.2143; Found: 521.2178.

*4.2.10. N-(2-((2,4-dimethoxyphenyl)amino)pyridin-3-yl)-1-(3-methoxybenzyl)-1H-1,2,3-triazole-4-carboxamide (**7j**)*

White solid, Yield 81%, M.P: 129−131 °C; ^{1}H NMR (500 MHz, CDCl$_3$) δ 8.71 (s, 1H), 8.13 (dd, J_1 = 4.9 Hz, J_2 = 1.7 Hz, 1H), 8.08 (s, 1H), 7.86 (dd, J_1 = 11.3 Hz, J_2 = 5.0 Hz, 2H), 7.35 – 7.30 (m, 1H), 6.93 (dd, J_1 = 8.1 Hz, J_2 = 2.2 Hz, 1H), 6.89 (d, J = 7.6 Hz, 1H), 6.85 – 6.80 (m, 3H), 6.51 – 6.47 (m, 2H), 5.55 (s, 2H), 3.81 (s, 6H), 3.79 (s, 3H); ^{13}C NMR (75 MHz, CDCl$_3$) δ 160.27, 158.93, 155.35, 150.33, 150.27, 145.44, 143.18, 134.98, 132.66, 130.49, 125.92, 123.68, 120.49, 119.88, 115.17, 114.51, 114.13, 103.95, 102.67, 99.06, 55.83, 55.61, 55.37, 54.65; MS (ESI): m/z 461 [M+H]$^+$; HRMS (ESI) Calcd for C$_{29}$H$_{26}$N$_5$O$_3$ [M+H]$^+$ 461.1932; Found: 461.1952.

*4.2.11. N-(2-((2,4-dimethoxyphenyl)amino)pyridin-3-yl)-1-(4-methoxybenzyl)-1H-1,2,3-triazole-4-carboxamide (**7k**)*

Light brown solid, Yield 80%, M.P: 168−170 °C; ^{1}H NMR (500 MHz, CDCl$_3$) δ 8.70 (s, 1H), 8.12 (dd, J_1 = 4.9 Hz, J_2 = 1.7 Hz, 1H), 8.04 (s, 1H), 7.89 – 7.82 (m, 2H), 7.30 – 7.26 (m, 2H), 6.95 – 6.90 (m, 2H), 6.81 (dd, J_1 = 7.6 Hz, J_2 = 5.0 Hz, 2H), 6.51 – 6.47 (m, 2H), 5.52 (s, 2H), 3.82 (s, 3H), 3.80 (s, 3H), 3.79 (s, 3H); ^{13}C NMR (75 MHz, CDCl$_3$) δ 160.26, 159.00, 155.31, 150.27, 145.43, 143.05, 132.70, 130.00, 125.69, 125.50, 123.62, 120.51, 119.84, 115.15, 114.72, 114.24, 103.88, 99.02, 55.81, 55.61, 55.41, 54.27; MS (ESI): m/z 461 [M+H]$^+$; HRMS (ESI) Calcd for C$_{29}$H$_{26}$N$_5$O$_3$ [M+H]$^+$ 461.1932; Found: 461.1961.

*4.2.12. N-(2-((2,4-dimethoxyphenyl)amino)pyridin-3-yl)-1-(4-fluorobenzyl)-1H-1,2,3-triazole-4-carboxamide (**7l**)*

White solid, Yield 83%, M.P: 192−194 °C; ^{1}H NMR (500 MHz, CDCl$_3$) δ 8.70 (s, 1H), 8.13 (dd, J_1 = 4.9 Hz, J_2 = 1.5 Hz, 1H), 8.09 (s, 1H), 7.87 (dd, J_1 = 7.7 Hz, J_2 = 1.5 Hz, 1H), 7.84 (d, J =

8.4 Hz, 1H), 7.35 – 7.30 (m, 2H), 7.14 – 7.08 (m, 2H), 6.85 – 6.79 (m, 2H), 6.53 – 6.47 (m, 2H), 5.57 (s, 2H), 3.80 (s, 3H), 3.79 (s, 3H); ^{13}C NMR (75 MHz, CDCl$_3$) δ 158.86, 155.38, 150.33, 150.25, 145.49, 132.65, 131.27, 130.29 (d, J_{C-F} = 8.4 Hz), 129.56, 125.79, 123.65, 120.54, 119.86, 116.57, 116.28, 115.21, 103.98, 99.08, 55.83, 55.61, 53.95; MS (ESI): m/z 449 [M+H]$^+$; HRMS (ESI) Calcd for C$_{29}$H$_{26}$N$_5$O$_3$ [M+H]$^+$ 449.1732; Found: 449.1758.

4.2.13. N-(2-((3,4-dimethoxyphenyl)amino)pyridin-3-yl)-1-(3-phenoxybenzyl)-1H-1,2,3-triazole-4-carboxamide (7m)

Light yellow solid, Yield 77%, M.P: 155−157 °C; ^{1}H NMR (300 MHz, CDCl$_3$) δ 8.79 (s, 1H), 8.13 (dd, J_1 = 4.8 Hz, J_2 = 1.5 Hz, 1H), 8.07 (s, 1H), 7.76 (dd, J_1 = 7.7 Hz, J_2 = 1.4 Hz, 1H), 7.40 – 7.30 (m, 3H), 7.14 (t, J = 7.4 Hz, 1H), 7.04 – 6.92 (m, 6H), 6.83 (ddd, J_1 = 18.2 Hz, J_2 = 12.0 Hz, J_3 = 5.5 Hz, 4H), 5.52 (s, 2H), 3.83 (s, 6H); ^{13}C NMR (125 MHz, CDCl$_3$) δ 158.89, 158.36, 156.24, 150.54, 149.15, 145.86, 144.98, 142.97, 135.32, 134.17, 133.01, 130.75, 129.98, 125.96, 124.04, 122.61, 119.56, 119.40, 118.90, 118.23, 115.42, 112.89, 111.75, 105.96, 56.19, 55.84, 54.36; MS (ESI): m/z 523 [M+H]$^+$; HRMS (ESI) Calcd for C$_{29}$H$_{26}$N$_5$O$_3$ [M+H]$^+$ 523.2088; Found: 523.2111.

4.2.14. N-(2-((3,4-dimethoxyphenyl)amino)pyridin-3-yl)-1-(3-methoxybenzyl)-1H-1,2,3-triazole-4-carboxamide (7n)

Yellow solid, Yield 85%, M.P: 160−162 °C; ^{1}H NMR (500 MHz, CDCl$_3$) δ 8.77 (s, 1H), 8.14 (dd, J_1 = 4.8 Hz, J_2 = 1.5 Hz, 1H), 8.07 (s, 1H), 7.76 (dd, J_1 = 7.7 Hz, J_2 = 1.4 Hz, 1H), 7.33 (t, J = 7.9 Hz, 1H), 6.98 (d, J = 2.3 Hz, 1H), 6.93 (dd, J_1 = 8.3 Hz, J_2 = 2.3 Hz, 1H), 6.89 (d, J = 7.6 Hz, 1H), 6.85 (ddd, J_1 = 7.4 Hz, J_2 = 6.7 Hz, J_3 = 2.6 Hz, 3H), 6.81 – 6.76 (m, 2H), 5.55 (s, 2H), 3.84 (d, J = 2.5 Hz, 6H), 3.81 (s, 3H); ^{13}C NMR (75 MHz, CDCl$_3$) δ 160.25, 158.95, 150.57, 149.12, 145.85, 144.94, 142.90, 134.87, 134.17, 133.06, 130.52, 125.98, 120.50, 119.56, 115.40, 114.48, 114.19, 112.87, 111.71, 105.92, 56.20, 55.85, 55.38, 54.67; MS (ESI): m/z 461 [M+H]$^+$; HRMS (ESI) Calcd for C$_{29}$H$_{26}$N$_5$O$_3$ [M+H]$^+$ 461.1932; Found: 461.1947.

4.2.15.   1-(3-Phenoxybenzyl)-N-(2-((3,4,5-trimethoxyphenyl)amino)pyridin-3-yl)-1H-1,2,3-triazole-4-carboxamide (7o)

Brown solid, Yield 83%, M.P: 118−120 °C; ^{1}H NMR (300 MHz, CDCl$_3$) δ 8.79 (s, 1H), 8.18 (dd, J_1 = 4.9 Hz, J_2 = 1.6 Hz, 1H), 8.09 (s, 1H), 7.78 (dd, J_1 = 7.7 Hz, J_2 = 1.4 Hz, 1H), 7.36 (td, J = 8.0, 4.2 Hz, 3H), 7.15 (t, J = 7.4 Hz, 1H), 7.05 − 6.94 (m, 5H), 6.89 (dd, J_1 = 7.7 Hz, J_2 = 4.8 Hz, 1H), 6.87 (s, 1H), 6.61 (s, 2H), 5.55 (s, 2H), 3.82 (s, 6H), 3.79 (s, 3H); ^{13}C NMR (75 MHz, CDCl$_3$) δ 158.97, 158.35, 156.24, 153.35, 149.98, 145.82, 142.90, 136.84, 135.35, 133.19, 130.77, 130.00, 126.05, 124.06, 122.64, 120.17, 119.40, 118.91, 118.27, 115.96, 97.92, 60.94, 56.04, 54.38, 29.73; MS (ESI): m/z 553 [M+H]$^+$; HRMS (ESI) Calcd for C$_{29}$H$_{26}$N$_5$O$_3$ [M+H]$^+$ 55.2194.; Found: 553.2224.

*4.2.16. 1-(3,4,5-Trimethoxybenzyl)-N-(2-((3,4,5-trimethoxyphenyl)amino)pyridin-3-yl)-1H-1,2,3-triazole-4-carboxamide (**7p**)*

Brown solid, Yield 76%, M.P: 110−112 °C; ^{1}H NMR (300 MHz, CDCl$_3$) δ 8.81 (s, 1H), 8.20 (dd, J_1 = 4.8 Hz, J_2 = 1.5 Hz, 1H), 8.11 (s, 1H), 7.85 − 7.76 (m, 1H), 6.91 (dd, J_1 = 7.7 Hz, J_2 = 4.9 Hz, 1H), 6.87 (s, 1H), 6.61 (s, 2H), 6.56 (s, 2H), 5.52 (s, 2H), 3.87 (d, J = 1.9 Hz, 9H), 3.83 (s, 6H), 3.80 (s, 3H); ^{13}C NMR (125 MHz, CDCl$_3$) δ 158.98, 153.92, 153.38, 149.87, 145.80, 142.82, 138.78, 136.83, 133.53, 133.07, 128.77, 125.87, 120.30, 116.06, 105.71, 97.93, 60.91, 56.28, 56.05, 55.07, 29.70; MS (ESI): m/z 551 [M+H]$^+$; HRMS (ESI) Calcd for C$_{29}$H$_{26}$N$_5$O$_3$ [M+H]$^+$ 551.2249; Found: 551.2277.

*4.2.17.   1-(4-Methoxybenzyl)-N-(2-((3,4,5-trimethoxyphenyl)amino)pyridin-3-yl)-1H-1,2,3-triazole-4-carboxamide (**7q**)*

Brown solid, Yield 80%, M.P: 130−132 °C; ^{1}H NMR (300 MHz, CDCl$_3$) δ 8.77 (s, 1H), 8.18 (dd, J_1 = 4.8 Hz, J_2 = 1.5 Hz, 1H), 8.02 (s, 1H), 7.76 (dd, J_1 = 7.7 Hz, J_2 = 1.3 Hz, 1H), 7.28 (d, J = 7.4 Hz, 2H), 6.93 (d, J = 8.6 Hz, 2H), 6.88 (dd, J_1 = 7.9 Hz, J_2 = 5.0 Hz, 1H), 6.85 (s, 1H), 6.60 (s, 2H), 5.52 (s, 2H), 3.82 (s, 3H), 3.81 (s, 6H), 3.78 (s, 3H); ^{13}C NMR (75 MHz, CDCl$_3$) δ 160.27, 159.08, 153.30, 150.00, 145.77, 142.70, 136.85, 133.24, 130.02, 125.81, 125.38, 120.12, 116.09, 115.89, 114.71, 97.84, 60.93, 56.02, 55.41, 54.29; MS (ESI): m/z 491 [M+H]$^+$; HRMS (ESI) Calcd for C$_{29}$H$_{26}$N$_5$O$_3$ [M+H]$^+$ 491.2037; Found: 491.2059.

*4.2.18.   1-(3-Methoxybenzyl)-N-(2-((3,4,5-trimethoxyphenyl)amino)pyridin-3-yl)-1H-1,2,3-triazole-4-carboxamide (**7r**)*

White solid, Yield 82%, M.P: 136−138℃; ^{1}H NMR (500 MHz, CDCl$_3$) δ 8.77 (s, 1H), 8.18 (dd, J_1 = 4.8 Hz, J_2 = 1.7 Hz, 1H), 8.07 (s, 1H), 7.77 (dd, J_1 = 7.8 Hz, J_2 = 1.6 Hz, 1H), 7.32 (dd, J_1 = 15.0 Hz, J_2 = 7.1 Hz, 1H), 6.93 (dd, J_1 = 8.3 Hz, J_2 = 2.1 Hz, 1H), 6.91 − 6.87 (m, 2H), 6.83 (s, 2H), 6.61 (s, 2H), 5.55 (s, 2H), 3.81 (s, 6H), 3.81 (s, 3H), 3.78 (s, 3H); ^{13}C NMR (125 MHz, CDCl$_3$) δ 160.27, 159.00, 153.35, 149.98, 145.81, 142.85, 136.85, 134.87, 133.49, 133.15, 130.53, 126.01, 120.49, 120.17, 118.35, 115.94, 114.46, 114.23, 97.94, 60.91, 56.04, 55.36, 54.66; MS (ESI): m/z 491 [M+H]$^+$; HRMS (ESI) Calcd for C$_{29}$H$_{26}$N$_5$O$_3$ [M+H]$^+$ 491.2037; Found: 491.2059.

4.2.19. 1-(4-Fluorobenzyl)-N-(2-((3,4,5-trimethoxyphenyl)amino)pyridin-3-yl)-1H-1,2,3-triazole-4-carboxamide (7s)

White solid, Yield 86%, M.P: 169−171 °C; ^{1}H NMR (500 MHz, CDCl$_3$) δ 8.76 (s, 1H), 8.18 (dd, J_1 = 4.8 Hz, J_2 = 1.7 Hz, 1H), 8.06 (s, 1H), 7.78 (dd, J_1 = 7.8 Hz, J_2 = 1.6 Hz, 1H), 7.32 (ddd, J_1 = 6.6 Hz, J_2 = 4.3 Hz, J_3 = 1.7 Hz, 2H), 7.14 − 7.08 (m, 2H), 6.89 (dd, J_1 = 7.8 Hz, J_2 = 4.9 Hz, 1H), 6.81 (s, 1H), 6.59 (s, 2H), 5.56 (s, 2H), 3.81 (s, 6H), 3.78 (s, 3H); ^{13}C NMR (100 MHz, CDCl$_3$) δ 163.14 (d, J_{C-F} = 249.5 Hz), 158.91, 153.38, 149.91, 145.80, 142.96, 136.83, 133.55, 133.15, 130.33 (d, J_{C-F} = 8.4 Hz), 129.40, 125.87, 120.25, 116.47 (d, J_{C-F} = 21.8 Hz), 116.04, 97.97, 60.94, 56.07, 53.99.; MS (ESI): m/z 479 [M+H]$^+$; HRMS (ESI) Calcd for C$_{29}$H$_{26}$N$_5$O$_3$ [M+H]$^+$ 479.1838; Found: 479.1859.

4.2.20. 1-(3-Phenoxybenzyl)-N-(2-(phenylamino)pyridin-3-yl)-1H-1,2,3-triazole-4-carboxamide (7t)

White solid, Yield 76%, M.P: 150−152 °C; ^{1}H NMR (300 MHz, CDCl$_3$) δ 8.79 (s, 1H), 8.18 (d, J = 4.7 Hz, 1H), 8.08 (s, 1H), 7.81 (d, J = 7.6 Hz, 1H), 7.43 − 7.22 (m, 7H), 7.20 − 7.11 (m, 1H), 7.10 − 6.81 (m, 8H), 5.54 (s, 2H); ^{13}C NMR (75 MHz, CDCl$_3$) δ 158.92, 158.37, 156.26, 149.65, 145.71, 142.97, 140.78, 135.35, 132.92, 130.77, 130.00, 128.94, 126.03, 124.06, 122.64, 122.18, 121.78, 120.35, 119.62, 119.43, 118.93, 118.25, 116.14, 54.38; MS (ESI): m/z 463 [M+H]$^+$; HRMS (ESI) Calcd for C$_{29}$H$_{26}$N$_5$O$_3$ [M+H]$^+$ 463.1877; Found: 463.1892.

4.2.21.   N-(2-(phenylamino)pyridin-3-yl)-1-(3,4,5-trimethoxybenzyl)-1H-1,2,3-triazole-4-carboxamide (7u)

White solid, Yield 75%, M.P: 142−144 °C; ^{1}H NMR (500 MHz, CDCl$_3$); δ 8.81 (s, 1H), 8.18 (dd, J_1 = 4.7 Hz, J_2 = 1.3 Hz, 1H), 8.09 (s, 1H), 7.82 (d, J = 7.7 Hz, 1H), 7.34 (d, J = 7.8 Hz, 2H), 7.28 (d, J = 7.5 Hz, 2H), 6.97 (t, J = 7.3 Hz, 1H), 6.92 (s, 1H), 6.89 (dd, J_1 = 7.8 Hz, J_2 = 4.9 Hz, 1H), 6.54 (s, 2H), 5.49 (s, 2H), 3.85 (s, 9H); ^{13}C NMR (125 MHz, CDCl$_3$); δ 158.96, 153.91, 149.59, 145.69, 142.91, 140.82, 138.74, 132.81, 128.93, 128.83, 125.91, 122.18, 120.44, 119.58, 116.18, 105.66, 60.91, 56.28, 55.04; MS (ESI): m/z 461 [M+H]$^+$; HRMS (ESI) Calcd for C$_{29}$H$_{26}$N$_5$O$_3$ [M+H]$^+$ 461.1932; Found: 461.1948.

4.2.22. 1-(3-Methoxybenzyl)-N-(2-(phenylamino)pyridin-3-yl)-1H-1,2,3-triazole-4-carboxamide (7v)

White solid, Yield 76%, M.P: 124−126 °C; ^{1}H NMR (500 MHz, CDCl$_3$) δ 8.79 (s, 1H), 8.18 (dd, J_1 = 4.8 Hz, J_2 = 1.7 Hz, 1H), 8.06 (s, 1H), 7.80 (dd, J_1 = 7.8 Hz, J_2 = 1.6 Hz, 1H), 7.36 − 7.31 (m, 3H), 7.29 − 7.26 (m, 2H), 6.99 − 6.95 (m, 1H), 6.93 (dd, J_1 = 8.6 Hz, J_2 = 2.6 Hz, 2H), 6.88 (dd, J_1 = 7.8 Hz, J_2 = 4.8 Hz, 2H), 6.84 − 6.81 (m, 1H), 5.54 (s, 2H), 3.80 (s, 3H); ^{13}C NMR (75 MHz, CDCl$_3$) δ 158.99, 149.69, 145.67, 142.89, 140.80, 134.90, 132.97, 130.51, 128.92, 126.04, 122.14, 120.51, 120.33, 119.61, 116.09, 114.49, 114.16, 55.38, 54.65; MS (ESI): m/z 401 [M+H]$^+$; HRMS (ESI) Calcd for C$_{29}$H$_{26}$N$_5$O$_3$ [M+H]$^+$ 401.1721; Found: 401.1748.

4.2.23. 1-(4-Methoxybenzyl)-N-(2-(phenylamino)pyridin-3-yl)-1H-1,2,3-triazole-4-carboxamide (7w)

White solid, Yield 79%, M.P: 145−147 °C; ^{1}H NMR (500 MHz, CDCl$_3$) δ 8.79 (s, 1H), 8.23 − 8.13 (m, 1H), 8.02 (s, 1H), 7.80 (dd, J_1 = 7.8 Hz, J_2 = 1.4 Hz, 1H), 7.34 (d, J = 7.7 Hz, 2H), 7.30 − 7.25 (m, 4H), 6.97 (t, J = 7.3 Hz, 1H), 6.93 (dd, J_1 = 6.7 Hz, J_2 = 1.9 Hz, 3H), 6.88 (dd, J_1 = 7.8 Hz, J_2 = 4.9 Hz, 1H), 5.51 (s, 2H), 3.82 (s, 3H); ^{13}C NMR (75 MHz, CDCl$_3$) δ 160.28, 159.04, 149.71, 145.66, 142.79, 140.81, 132.95, 130.03, 128.91, 125.78, 125.41, 122.12, 120.34, 119.60, 116.07, 114.73, 55.42, 54.29; MS (ESI): m/z 401 [M+H]$^+$; HRMS (ESI) Calcd for C$_{29}$H$_{26}$N$_5$O$_3$ [M+H]$^+$ 401.1721; Found: 401.1739.

4.2.24. 1-(4-Fluorobenzyl)-N-(2-(phenylamino)pyridin-3-yl)-1H-1,2,3-triazole-4-carboxamide (7x)

White solid, Yield 77%, M.P: 165−167 °C; ^{1}H NMR (500 MHz, CDCl$_3$) δ 8.79 (s, 1H), 8.18 (dd, J_1 = 4.8 Hz, J_2 = 1.6 Hz, 1H), 8.06 (s, 1H), 7.81 (dd, J_1 = 7.8 Hz, J_2 = 1.6 Hz, 1H), 7.32 (dd, J_1 = 15.6 Hz, J_2 = 6.8 Hz, 4H), 7.28 (d, J = 7.4 Hz, 2H), 7.13 − 7.07 (m, 2H), 6.97 (t, J = 7.3 Hz, 1H), 6.89 (dd, J_1 = 7.7 Hz, J_2 = 4.8 Hz, 2H), 5.55 (s, 2H); ^{13}C NMR (125 MHz, CDCl$_3$) δ 163.12 (d, J = 249.2 Hz), 158.91, 149.66, 145.68, 143.02, 140.82, 132.94, 130.33 (d, J = 8.4 Hz), 129.46, 128.94, 125.91, 122.19, 120.39, 119.61, 116.45 (d, J = 21.9 Hz), 116.15, 53.96; MS (ESI): m/z 389 [M+H]$^+$; HRMS (ESI) Calcd for C$_{29}$H$_{26}$N$_5$O$_3$ [M+H]$^+$ 389.1521; Found: 389.1548.

*4.2.25.   N-(2-((4-fluorophenyl)amino)pyridin-3-yl)-1-(3-phenoxybenzyl)-1H-1,2,3-triazole-4-carboxamide (**7y**)*

White solid, Yield 76%, M.P: 146−148 °C; ^{1}H NMR (500 MHz, CDCl$_3$) δ 8.77 (s, 1H), 8.16 (dd, J_1 = 4.9 Hz, J_2 = 1.6 Hz, 1H), 8.09 (s, 1H), 7.75 (dd, J_1 = 7.8 Hz, J_2 = 1.6 Hz, 1H), 7.39 − 7.33 (m, 3H), 7.31 (ddd, J_1 = 10.5 Hz, J_2 = 5.3 Hz, J_3 = 2.9 Hz, 2H), 7.15 (t, J = 7.4 Hz, 1H), 7.04 − 6.94 (m, 7H), 6.92 (s, 1H), 6.87 (dd, J_1 = 7.7 Hz, J_2 = 4.9 Hz, 1H), 5.56 (s, 2H).; ^{13}C NMR (125 MHz, CDCl$_3$) δ 158.92, 158.47 (d, $J_{\text{C-F}}$ = 240.7 Hz), 158.40, 156.25, 150.08, 145.82, 142.90, 136.69, 135.30, 133.11, 130.79, 130.01, 126.02, 124.07, 122.62, 121.78, 121.72, 119.76, 119.43, 118.95, 118.25, 115.86, 115.57, 115.39, 54.41; MS (ESI): m/z 481 [M+H]$^+$; HRMS (ESI) Calcd for C$_{29}$H$_{26}$N$_5$O$_3$ [M+H]$^+$ 481.1783; Found: 481.1799.

*4.2.26.   N-(2-((4-fluorophenyl)amino)pyridin-3-yl)-1-(3,4,5-trimethoxybenzyl)-1H-1,2,3-triazole-4-carboxamide (**7z**)*

White solid, Yield 75%, M.P: 190−192 °C; ^{1}H NMR (300 MHz, CDCl$_3$) δ 8.78 (s, 1H), 8.16 (dd, J_1 = 4.8 Hz, J_2 = 1.5 Hz, 1H), 8.09 (s, 1H), 7.75 (dd, J_1 = 7.7 Hz, J_2 = 1.4 Hz, 1H), 7.35 − 7.27 (m, 2H), 6.97 (dd, J_1 = 14.9 Hz, J_2 = 6.1 Hz, 3H), 6.88 (dd, J_1 = 7.7 Hz, J_2 = 4.9 Hz, 1H), 6.55 (s, 2H), 5.50 (s, 2H), 3.86 (s, 9H); ^{13}C NMR (125 MHz, CDCl$_3$) δ 158.96, 158.46 (d, $J_{\text{C-F}}$ = 240.8 Hz), 153.94, 150.01, 145.79, 142.83, 138.81, 136.72, 133.02, 128.77, 125.88, 121.71 (d, $J_{\text{C-F}}$ = 7.7 Hz), 119.86, 115.92, 115.48 (d, $J_{\text{C-F}}$ = 22.4 Hz), 105.72, 60.92, 56.30, 55.09; MS (ESI): m/z 479 [M+H]$^+$; HRMS (ESI) Calcd for C$_{29}$H$_{26}$N$_5$O$_3$ [M+H]$^+$ 479.1838; Found: 479.1853.

*4.2.27.   N-(2-((4-fluorophenyl)amino)pyridin-3-yl)-1-(4-methoxybenzyl)-1H-1,2,3-triazole-4-carboxamide (**7aa**)*

White solid, Yield 75%, M.P: 162−164 °C; ^{1}H NMR (300 MHz, CDCl$_3$) δ 8.80 (s, 1H), 8.16 (dd, J_1 = 4.8 Hz, J_2 = 1.6 Hz, 1H), 8.03 (s, 1H), 7.75 (dd, J_1 = 7.7 Hz, J_2 = 1.4 Hz, 1H), 7.36 − 7.30 (m, 2H), 7.28 (d, J = 2.9 Hz, 2H), 7.04 − 6.91 (m, 5H), 6.87 (dd, J_1 = 7.7 Hz, J_2 = 4.9 Hz, 1H), 5.53 (s, 2H), 3.84 (s, 3H); ^{13}C NMR (100MHz, CDCl$_3$) δ 160.32, 159.04, 158.42 (d, J_{C-F} = 240.7 Hz), 150.10, 145.75, 142.72, 136.70, 133.16, 130.04, 125.79, 125.36, 121.73 (d, J_{C-F} = 7.7 Hz), 119.76, 115.81, 115.46 (d, J_{C-F} = 22.4 Hz), 114.76, 55.43, 54.34; MS (ESI): *m/z* 419 [M+H]$^+$; HRMS (ESI) Calcd for C$_{29}$H$_{26}$N$_5$O$_3$ [M+H]$^+$ 419.1626; Found: 419.1641.

*4.2.28.   1-(4-Fluorobenzyl)-N-(2-((4-fluorophenyl)amino)pyridin-3-yl)-1H-1,2,3-triazole-4-carboxamide (**7ab**)*

White solid, Yield 78%, M.P: 186−188 °C; ^{1}H NMR (300 MHz, CDCl$_3$) δ 8.76 (s, 1H), 8.15 (dd, J_1 = 4.9 Hz, J_2 = 1.6 Hz, 1H), 8.06 (s, 1H), 7.74 (dd, J_1 = 7.8 Hz, J_2 = 1.5 Hz, 1H), 7.31 (ddd, J_1 = 9.0 Hz, J_2 = 5.4 Hz, J_3 = 2.2 Hz, 4H), 7.16 − 7.06 (m, 2H), 7.03 − 6.93 (m, 2H), 6.92 (s, 1H), 6.87 (dd, J_1 = 7.7 Hz, J_2 = 4.9 Hz, 1H), 5.56 (s, 2H); ^{13}C NMR (125 MHz, CDCl$_3$) δ 164.14, 162.16, 159.43, 158.88, 157.51, 150.04, 145.82, 142.96, 136.70, 133.09, 130.32 (d, J_{C-F} = 8.3 Hz), 129.40, 125.87, 121.72 (d, J_{C-F} = 7.6 Hz), 119.80, 116.49 (d, J_{C-F} = 21.9 Hz), 115.90, 115.48 (d, J_{C-F} = 22.4 Hz), 54.01; MS (ESI): *m/z* 407.1426 [M+H]$^+$; HRMS (ESI) Calcd for C$_{29}$H$_{26}$N$_5$O$_3$ [M+H]$^+$ 493.1983; Found: 407.1452.

*4.2.29.   N-(2-((4-fluorophenyl)amino)pyridin-3-yl)-1-(3-methoxybenzyl)-1H-1,2,3-triazole-4-carboxamide (**7ac**)*

White solid, Yield 79%, M.P: 165−167 °C; ^{1}H NMR (500 MHz, CDCl$_3$) δ 8.77 (s, 1H), 8.15 (dd, J_1 = 4.9 Hz, J_2 = 1.7 Hz, 1H), 8.06 (s, 1H), 7.74 (dd, J_1 = 7.8 Hz, J_2 = 1.6 Hz, 1H), 7.35 − 7.32 (m, 1H), 7.32 − 7.29 (m, 2H), 7.00 − 6.95 (m, 2H), 6.94 (s, 1H), 6.94 − 6.91 (m, 1H), 6.89 (d, J = 7.5 Hz, 1H), 6.86 (dd, J_1 = 7.7 Hz, J_2 = 4.9 Hz, 1H), 6.84 − 6.81 (m, 1H), 5.55 (s, 2H), 3.81 (s, 3H); ^{13}C NMR (75 MHz, CDCl$_3$) δ 160.27, 160.04, 158.97, 156.84, 150.07, 145.77, 142.84, 136.69, 134.83, 133.14, 130.55, 121.74 (d, J_{C-F} = 7.7 Hz), 120.51, 119.74, 115.83, 115.47 (d, J_{C-F} = 22.4 Hz), 114.49, 114.21, 55.38, 54.70; MS (ESI): *m/z* 419 [M+H]$^+$; HRMS (ESI) Calcd for C$_{29}$H$_{26}$N$_5$O$_3$ [M+H]$^+$ 419.1626; Found: 419.1650.

*4.2.30.   N-(2-((4-hydroxyphenyl)amino)pyridine-3-yl)-1-(3-phenoxybenzyl)-1H-1,2,3-triazole-4-carboxamide (**7ad**)*

Light brown solid, Yield 74%, M.P: 196−198 °C; ^{1}H NMR (300 MHz, CDCl$_3$ + DMSO-d_6) δ 9.89 (s, 1H), 8.83 (s, 1H), 8.61 (s, 1H), 8.37 (d, J = 3.6 Hz, 1H), 8.09 (d, J = 7.4 Hz, 1H), 7.81 (s, 1H), 7.69 (dd, J_1 = 9.2 Hz, J_2 = 6.1 Hz, 4H), 7.55 (d, J = 8.6 Hz, 2H), 7.47 (t, J = 7.4 Hz, 1H), 7.43 – 7.22 (m, 6H), 7.09 (dd, J_1 = 10.8 Hz, J_2 = 5.7 Hz, 3H), 5.92 (s, 2H); ^{13}C NMR (100 MHz, CDCl$_3$) δ 158.32, 156.52, 155.33, 151.48, 149.79, 143.52, 142.19, 135.68, 132.50, 131.77, 129.37, 128.84, 125.94, 122.65, 121.76, 121.15, 118.25, 117.88, 117.42, 117.25, 114.22, 112.85, 52.52; MS (ESI): m/z 479 [M+H]$^+$; HRMS (ESI) Calcd for C$_{29}$H$_{26}$N$_5$O$_3$ [M+H]$^+$ 479.1826; Found: 479.1844.

4.2.31.   N-(2-((4-hydroxyphenyl)amino)pyridin-3-yl)-1-(3,4,5-trimethoxybenzyl)-1H-1,2,3-triazole-4-carboxamide (7ae)

Light brown solid, Yield 73%, M.P: 191−193 °C; ^{1}H NMR (300 MHz, CDCl$_3$ + DMSO-d_6) δ 9.86 (s, 1H), 8.69 (s, 1H), 8.55 (s, 1H), 7.97 (d, J = 2.8 Hz, 1H), 7.73 (d, J = 7.7 Hz, 2H), 7.30 – 7.18 (m, 2H), 6.72 (dd, J_1 = 9.5 Hz, J_2 = 7.0 Hz, 5H), 5.56 (s, 2H), 3.84 (d, J = 2.5 Hz, 6H), 3.76 (d, J = 2.7 Hz, 3H); ^{13}C NMR (100 MHz, CDCl$_3$ + DMSO-d_6) δ 158.81, 152.95, 152.08, 150.28, 144.35, 142.66, 137.59, 132.88, 132.17, 129.13, 125.99, 121.81, 118.69, 114.88, 113.56, 105.11, 60.06, 55.59, 53.96; MS (ESI): m/z 477 [M+H]$^+$; HRMS (ESI) Calcd for C$_{29}$H$_{26}$N$_5$O$_3$ [M+H]$^+$ 477.1881; Found: 477.1898.

4.2.32.   N-(2-((4-hydroxyphenyl)amino)pyridin-3-yl)-1-(3-methoxybenzyl)-1H-1,2,3-triazole-4-carboxamide (7af)

Light brown solid, Yield 77%, M.P: 175−177 °C; ^{1}H NMR (400 MHz, CDCl$_3$) δ 9.56 (s, 1H), 8.56 (s, 1H), 8.29 (d, J = 4.8 Hz, 1H), 8.03 (d, J = 6.7 Hz, 1H), 7.77 (t, J = 8.2 Hz, 1H), 7.39 (s, 1H), 7.35 – 7.17 (m, 3H), 6.97 – 6.83 (m, 3H), 6.77 (d, J = 8.5 Hz, 3H), 5.58 (s, 2H), 3.80 (s, 3H); ^{13}C NMR (100 MHz, CDCl$_3$) δ 159.25, 158.66, 151.97, 150.13, 143.95, 142.55, 135.09, 132.79, 132.02, 129.48, 126.02, 125.89, 121.70, 119.63, 118.64, 114.73, 113.37, 113.28, 54.56, 53.41; MS (ESI): m/z 417 [M+H]$^+$; HRMS (ESI) Calcd for C$_{29}$H$_{26}$N$_5$O$_3$ [M+H]$^+$ 417.1670; Found: 417.1683.

4.2.33.   N-(2-((4-hydroxyphenyl)amino)pyridin-3-yl)-1-(4-methoxybenzyl)-1H-1,2,3-triazole-4-carboxamide (7ag)

Light brown solid, Yield 79%, M.P: 170−172 °C; ^{1}H NMR (300 MHz, CDCl$_3$ + DMSO-d_6) δ 9.87 (s, 1H), 8.74 (s, 1H), 8.55 (s, 1H), 7.95 (d, J = 3.4 Hz, 1H), 7.81 (s, 1H), 7.70 (d, J = 7.6 Hz, 1H), 7.35 (d, J = 8.6 Hz, 2H), 7.24 (d, J = 8.7 Hz, 2H), 6.90 (d, J = 8.6 Hz, 2H), 6.76 − 6.64 (m, 3H), 5.58 (s, 2H), 3.78 (s, 3H); ^{13}C NMR (100 MHz, CDCl$_3$) δ 164.69, 164.26, 157.44, 155.70, 149.54, 148.03, 138.37, 137.66, 134.70, 131.27, 131.19, 127.13, 124.18, 120.22, 119.24, 118.86, 60.13, 58.56; MS (ESI): m/z 417 [M+H]$^+$; HRMS (ESI) Calcd for C$_{29}$H$_{26}$N$_5$O$_3$ [M+H]$^+$ 417.1670; Found: 417.1683.

*4.2.34.   1-(4-Fluorobenzyl)-N-(2-((4-hydroxyphenyl)amino)pyridin-3-yl)-1H-1,2,3-triazole-4-carboxamide (**7ah**)*

Light brown solid, Yield 80%, M.P: 204−206 °C; ^{1}H NMR (300 MHz, CDCl$_3$ + DMSO-d_6) δ 9.88 (s, 1H), 8.65 (dd, J_1 = 32.2 Hz, J_2 = 7.1 Hz, 2H), 7.96 (d, J = 6.5 Hz, 1H), 7.80 − 7.66 (m, 2H), 7.49 − 7.36 (m, 2H), 7.24 (d, J = 8.7 Hz, 2H), 7.11 (t, J = 8.6 Hz, 2H), 6.72 (dd, J_1 = 12.4 Hz, J_2 = 6.8 Hz, 3H), 5.65 (s, 2H); ^{13}C NMR (100 MHz, CDCl$_3$) δ 168.72, 166.26, 164.18, 157.46, 155.70, 149.68, 148.16, 138.36, 137.63, 135.16 (d, J_{C-F} = 8.2 Hz), 131.48 (d, J_{C-F} = 11.3 Hz), 127.16, 124.12, 120.79 (d, J_{C-F} = 21.5 Hz), 120.24, 118.89, 58.20; MS (ESI): m/z 405 [M+H]$^+$; HRMS (ESI) Calcd for C$_{29}$H$_{26}$N$_5$O$_3$ [M+H]$^+$ 405.1470; Found: 405.1488.

*4.2.35.   1-Benzyl-N-(2-((4-fluorophenyl)amino)pyridin-3-yl)-1H-1,2,3-triazole-4-carboxamide (**7ai**)*

White solid, Yield 81%, M.P: 158−160 °C; ^{1}H NMR (300 MHz, CDCl$_3$) δ 8.81 (s, 1H), 8.18 (dd, J_1 = 4.8 Hz, J_2 = 1.4 Hz, 1H), 8.07 (s, 1H), 7.86 − 7.72 (m, 1H), 7.38 − 7.27 (m, 5H), 7.26 − 7.19 (m, 1H), 7.10 (t, J = 8.5 Hz, 2H), 6.97 (t, J = 7.2 Hz, 1H), 6.92 (s, 1H), 6.89 (dd, J_1 = 7.7 Hz, J_2 = 4.9 Hz, 1H), 5.55 (s, 2H); ^{13}C NMR (125MHz, CDCl$_3$) δ 163.12 (d, J_{C-F} = 249.3 Hz), 158.88, 149.65, 145.71, 143.02, 140.81, 132.89, 130.31 (d, J_{C-F} = 8.3 Hz), 128.93, 125.88, 122.17, 120.84, 120.36, 119.58, 116.45 (d, J_{C-F} = 21.9 Hz), 116.15, 53.95; MS (ESI): m/z 389 [M+H]$^+$; HRMS (ESI) Calcd for C$_{29}$H$_{26}$N$_5$O$_3$ [M+H]$^+$ 389.1521; Found: 389.1517.

*4.2.36.   1-Benzyl-N-(2-((3,4,5-trimethoxyphenyl)amino)pyridin-3-yl)-1H-1,2,3-triazole-4-carboxamide (**7aj**)*

White Brown solid, Yield 79%, M.P: 160−162 °C; ^{1}H NMR (300 MHz, CDCl$_3$) δ 8.84 (s, 1H), 8.20 (dd, J_1 = 4.8 Hz, J_2 = 1.5 Hz, 1H), 8.11 (s, 1H), 7.89 – 7.72 (m, 1H), 7.39 – 7.31 (m, 2H), 7.26 (dt, J = 14.2, 6.3 Hz, 2H), 7.00 (dd, J_1 = 9.9 Hz, J_2 = 4.3 Hz, 1H), 6.95 (s, 1H), 6.91 (dd, J_1 = 7.8 Hz, J_2 = 4.9 Hz, 1H), 6.56 (s, 2H), 5.51 (s, 2H), 3.87 (s, 9H). ^{13}C NMR (125 MHz, CDCl$_3$) δ 158.98, 153.89, 149.61, 145.68, 142.89, 140.83, 138.71, 132.85, 128.93, 125.91, 122.15, 120.82, 120.43, 119.55, 116.17, 105.65, 60.91, 56.27, 55.0; MS (ESI): m/z 461 [M+H]$^+$; HRMS (ESI) Calcd for C$_{29}$H$_{26}$N$_5$O$_3$ [M+H]$^+$ 461.1932; Found: 461.1938.

4.2.37. *1-Benzyl-N-(2-((4-methoxyphenyl)amino)pyridin-3-yl)-1H-1,2,3-triazole-4-carboxamide (7ak)*

White solid, Yield 78%, M.P: 145−147 °C; ^{1}H NMR (500 MHz, CDCl$_3$) δ 8.80 (s, 1H), 8.17 (dd, J_1 = 4.8 Hz, J_2 = 1.6 Hz, 1H), 8.02 (s, 1H), 7.79 (dd, J_1 = 7.8 Hz, J_2 = 1.6 Hz, 1H), 7.34 (dt, J = 7.6, 3.9 Hz, 2H), 7.29 – 7.24 (m, 4H), 7.00 – 6.94 (m, 2H), 6.94 – 6.91 (m, 2H), 6.88 (dd, J_1 = 7.8 Hz, J_2 = 4.8 Hz, 1H), 5.51 (s, 2H), 3.82 (s, 3H); ^{13}C NMR (75 MHz, CDCl$_3$) δ 160.28, 159.04, 149.71, 145.65, 142.78, 140.81, 132.96, 130.02, 128.90, 125.78, 122.11, 120.85, 120.32, 119.60, 116.05, 114.72, 55.40, 54.27; MS (ESI): m/z 401 [M+H]$^+$; HRMS (ESI) Calcd for C$_{29}$H$_{26}$N$_5$O$_3$ [M+H]$^+$ 401.1721; Found: 401.1719.

4.2.38. *1-Benzyl-N-(2-((3-methoxyphenyl)amino)pyridin-3-yl)-1H-1,2,3-triazole-4-carboxamide (7al)*

White solid, Yield 80%, M.P: 120−122 °C; ^{1}H NMR (400 MHz, CDCl$_3$) δ 8.80 (s, 1H), 8.17 (dd, J_1 = 4.8 Hz, J_2 = 1.5 Hz, 1H), 8.06 (s, 1H), 7.77 (ddd, J_1 = 26.5 Hz, J_2 = 7.8 Hz, J_3 = 1.5 Hz, 1H), 7.32 (ddd, J_1 = 22.1 Hz, J_2 = 10.7 Hz, J_3 = 5.4 Hz, 4H), 7.25 – 7.19 (m, 1H), 6.96 (dd, J_1 = 11.6 Hz, J_2 = 4.2 Hz, 1H), 6.92 (dd, J_1 = 8.2 Hz, J_2 = 6.2 Hz, 2H), 6.88 (dd, J_1 = 7.7 Hz, J_2 = 4.8 Hz, 2H), 6.83 (d, J = 1.9 Hz, 1H), 5.54 (s, 2H), 3.80 (s, 3H); ^{13}C NMR (75 MHz, CDCl$_3$) δ 160.24, 158.99, 149.68, 145.65, 142.90, 140.80, 134.90, 132.95, 130.51, 128.92, 126.04, 122.14, 120.87, 120.51, 119.62, 116.09, 114.49, 114.17, 55.38, 54.65; MS (ESI): m/z 401 [M+H]$^+$; HRMS (ESI) Calcd for C$_{29}$H$_{26}$N$_5$O$_3$ [M+H]$^+$ 401.1721; Found: 401.1714.

4.3. Biology

4.3.1. Anticancer activity

The Anticancer activity of the compounds was determined using MTT assay [52]. 1×10^4 cells/well were seeded in 100µl DMEM (Dulbecco's Modified Eagle's medium)/MEM (Minimum Essential Medium), supplemented with 10% FBS in each well of 96-well micro culture plates and incubated for 24 h at 37°C in a CO_2 incubator. After 24 h of incubation, all the synthesized compounds were added to the cells and incubated for 48 h. After 48 h of drug treatment, 10 µl MTT (3-(4, 5-dimethylthiazol-2-yl)- 2,5-diphenyl tetrazolium bromide) (5 mg/mL) was added to each well and the plates were further incubated for 4 h. Then the supernatant from each well was carefully removed, formazon crystals were dissolved in 100 µl of DMSO and absorbance at 570 nm wavelength was recorded.

4.3.2. Cell cycle analysis

Flow cytometric analysis (FACS) was performed to evaluate the distribution of the cells through the cell cycle phases. A549 cells were treated with compound **7f** at 1 and 2 µM concentrations for 48 h. Untreated and treated cells were harvested, washed with phosphate buffered saline (PBS), fixed in ice-cold 70% ethanol, and stained with propidium iodide (Sigma–Aldrich). Cell cycle analysis was performed by flow cytometry (Becton Dickinson FACS Caliber instrument) [53].

4.3.3. Tubulin polymerization assay

A fluorescence based in vitro tubulin polymerization assay was performed according to the manufacturer's protocol (BK011, Cytoskeleton, Inc.). Briefly, the reaction mixture in a total volume of 10 µL contained PEM buffer, GTP (1 µM) in the presence or absence of test compounds (final concentration of 3 µM). Tubulin polymerization was followed by a time dependent increase in fluorescence due to the incorporation of a fluorescence reporter into microtubules as polymerization proceeds. Fluorescence emission at 420 nm (excitation wavelength is 360 nm) was measured by using a Varioscan multimode plate reader (Thermo scientific Inc.). Nocodazole was used as reference compound. The IC50 value was defined as the drug concentration required inhibiting 50% of tubulin assembly compared to control. The reaction mixture for these experiments include: tubulin (3 mg/ml) in PEM buffer, GTP (1 µM), in the presence or absence of test compounds at varying concentrations. Polymerization was monitored by increase in the fluorescence as mentioned above at 37 °C [54, 44].

4.3.4. Hoechst staining

A549 cells were seeded at a density of 10,000 cells over 18 mm cover slips and incubated for 24 h. After incubation, cells were treated with the compound **7f** at 1 and 2 µM concentration for 48 h. Hoechst 33258 (Sigma Aldrich) was added to the cells at a concentration of 0.5 mg/mL and

incubated for 30 min at 37 °C. Later, the cells were washed with phosphate buffered saline (PBS). Cells from each cover slip were captured from randomly selected fields under fluorescent microscope (Olympus microscope) to qualitatively determine the proportion of viable and apoptotic cells based on their relative fluorescence and nuclear fragmentation [55].

4.3.5. Measurement of mitochondrial membrane potential (ΔΨm)

A549 (1×10^6 cells/well) cells were cultured in six-well plates. After plating, cells were treated with compound **7f** at 1 and 2 μM concentrations for 48 h. After 48 h of treatment, cells were collected by trypsinization and washed with PBS followed by resuspending in JC-1 (5,5,6,6-tetrachloro-1,1,3,3-tetraethylbenzimidazolocarbocyanine iodide) and incubated at 37 ^{0}C for 15 min. The cells were then subjected to flow cytometric analysis on a flow cytometer (Becton Dickinson) in the FL1, FL2 channel to detect mitochondrial potential [56].

4.3.6. Annexin V-FITC assay for apoptosis

A549 (1×10^6) cells were seeded in six-well plates and allowed to grow overnight. The medium was then replaced with complete medium containing compound **7f** at 1 and 2 μM concentrations for 48 h. After 48 h of drug treatment, cells from the supernatant and adherent monolayer cells were harvested by trypsinization, washed with PBS at 5000 rpm. Then the cells were stained with Annexin VFITC and propidium iodide using the Annexin-V-FITC apoptosis detection kit (Sigma Aldrich). Then the samples were analyzed by flowcytometry as described earlier [57].

Acknowledgements

References

[1]   A. Jordan, J. A. Hadfield, N. J. Lawrence, A. T. McGown, Tubulin as a target for anticancer drugs: agents which interact with the mitotic spindle, Med. Research Rev. 18 (1998) 259−296.

[2]   C. Dumontet, M. A. Jordan, Microtubule-binding agents: a dynamic field of cancer therapeutics, Nat. Rev. Drug Discovery, 9 (2010) 790−803.

[3]   (a) M. Kavallaris, Microtubules and resistance to tubulin-binding agents, Nat. Rev. Cancer, 10 (2010) 194−204. (b) J. Mccarroll, A. Parker, M. Kavallaris, Microtubules and their role in cellular stress in cancer. Front. Oncol. 4 (2014) 1−19.

[4]   A. E. Prota, K. Bargsten, D. Zurwerra, J. J. Field, J. F. Díaz, K.-H. Altmann, M. O. Steinmetz, Molecular mechanism of action of microtubule-stabilizing anticancer agents, Science, 339 (2013) 587−590.

[5]   E. Nogales, Structural insights into microtubule function, Annual Rev. Biochem. 69 (2000) 277−302.

[6]   S. L. Kline-Smith, C. E. Walczak, Mitotic spindle assembly and chromosome segregation: refocusing on microtubule dynamics, Mol. Cell, 15 (2004) 317−327.

[7]   C. C. Rohena, S. L. Mooberry, Recent progress with microtubule stabilizers: new compounds, binding modes and cellular activities, Nat. Prod. Rep. 31 (2014) 335−355.

[8]   R. Kaur, G. Kaur, R. K. Gill, R. Soni, J. Bariwal, Recent developments in tubulin polymerization inhibitors: An overview, Eur. J. Med. Chem. 87 (2014) 89−124.

[9]   B. Bhattacharyya, D. Panda, S. Gupta, M. Banerjee, Anti- mitotic activity of colchicine and the structural basis for its interaction with tubulin, Med. Res. Rev. 28 (2008) 155−183.

[10]   S.-M. Chen, L.-H. Ding, J. Meng, New microtubule-inhibiting anticancer agents, Exp. Opinion on Invest. Drugs, 19 (2010) 329−343.

[11]   N. Mahindroo, J.-P. Liou, J.-Y. Chang, H.-P. Hsieh, Antitubulin agents for the treatment of cancer–a medicinal chemistry update, Exp. Opinion on Ther. Patents, 16 (2006) 647−691.

[12]   M. Jordan, Mechanism of action of antitumor drugs that interact with microtubules and tubulin, Curr. Med. Chem. Anti-Cancer Agents, 2 (2002) 1−17.

[13]   M. Zweifel, G. C. Jayson, N. Reed, R. Osborne, B. Hassan, J. Ledermann, G. Shreeves, L. Poupard, S.-P. Lu, J. Balkissoon, Phase II trial of combretastatin A4 phosphate, carboplatin, and paclitaxel in patients with platinum-resistant ovarian cancer, Annals of oncology, 22 (2011) 2036−2041.

[14]   D. M. Chase, D. J. Chaplin, B. J. Monk, The development and use of vascular targeted therapy in ovarian cancer, Gynecologic Oncology 2017.

[15]   B. C. Baguley, M. J. McKeage, Anticancer potential of tumor vascular disrupting agents: review of the latest clinical evidence. Clinical Investigation, 2 (2012) 985−993.

[16]   M.-J. Pérez-Pérez, E.-M. Priego, O. Bueno, M. S. Martins, M.-D. Canela, S. Liekens, Blocking blood flow to solid tumors by destabilizing tubulin: an approach to targeting tumor growth, J. Med. Chem. 59 (2016) 8685−8711.

[17]   R. Kaur, G. Kaur, R. K. Gill, R. Soni, J. Bariwal, Recent developments in tubulin polymerization inhibitors: an overview, Eur. J. Med. Chem. 87 (2014) 89−124.

[18]   D. W. Siemann, The unique characteristics of tumor vasculature and preclinical evidence for its selective disruption by tumor-vascular disrupting agents, Cancer Treatment Rev. 37 (2011) 63−74.

[19]   G. M. Tozer, C. Kanthou, B. C. Baguley, Disrupting tumour blood vessels, Nat. Rev. Cancer, 5 (2005) 423−435.

[20]   N. Koyanagi, T. Nagasu, F. Fujita, T. Watanabe, K. Tsukahara, Y. Funahashi, M. Fujita, T. Taguchi, H. Yoshino, K. Kitoh, In vivo tumor growth inhibition produced by a novel sulfonamide, E7010, against rodent and human tumors. Cancer Research, 54, (1994) 1702−1706.

[21]   K. Yoshimatsu, A. Yamaguchi, H. Yoshino, N. Koyanagi, K. Kitoh, Mechanism of action of E7010, an orally active sulfonamide antitumor agent: inhibition of mitosis by binding to the colchicine site of tubulin, Cancer Research, 57 (1997) 3208−3213.

[22]   A. Dorléans, B. Gigant, R. B. Ravelli, P. Mailliet, V. Mikol, M. Knossow, Variations in the colchicine-binding domain provide insight into the structural switch of tubulin. Proceedings of the National Academy of Sciences, 106 (2009) 13775−13779.

[23]   M.-J. Lai, H.-Y. Lee, H.-Y. Chuang, L.-H. Chang, A.-C. Tsai, M.-C. Chen, H.-L. Huang, Y.-W. Wu, C.-M. Teng, S.-L. Pan, N-Sulfonyl-aminobiaryls as antitubulin agents and inhibitors of signal transducers and activators of transcription 3 (STAT3) signaling, J. Med. Chem. 58 (2015) 6549−6558.

[24]   Z. Segaoula, J. Leclercq, V. Verones, N. Flouquet, M. Lecoeur, L. Ach, N. Renault, A. Barczyk, P. Melnyk, P. Berthelot, Synthesis and biological evaluation of N-[2-(4-Hydroxyphenylamino)-pyridin-3-yl]-4-methoxy-benzenesulfonamide (ABT-751) tricyclic analogues as antimitotic and antivascular agents with potent in vivo antitumor activity, J. Med. Chem. 59 (2016) 8422−8440.

[25]   S. X. Cai, B. Nguyen, S. Jia, J. Herich, J. Guastella, S. Reddy, B. Tseng, J. Drewe, S. Kasibhatla, Discovery of substituted N-phenyl nicotinamides as potent inducers of apoptosis using a cell-and caspase-based high throughput screening assay, J. med. Chem. 46 (2003) 2474−2481.

[26]   H.-Y. Lee, S.-L. Pan, M.-C. Su, Y.-M. Liu, C.-C. Kuo, Y.-T. Chang, J.-S. Wu, C.-Y. Nien, S. Mehndiratta, C.-Y. Chang, Furanylazaindoles: potent anticancer agents in vitro and in vivo, J. Med. Chem. 56 (2013) 8008−8018.

[27]   G. Dong, W. Chen, X. Wang, X. Yang, T. Xu, P. Wang, W. Zhang, Y. Rao, C. Miao, C. Sheng, Small Molecule Inhibitors Simultaneously Targeting Cancer Metabolism and Epigenetics: Discovery of Novel Nicotinamide Phosphoribosyltransferase (NAMPT) and Histone Deacetylase (HDAC) Dual Inhibitors, J. Med. Chem. 60 (2017) 7965−7983.

[28]   L.-D. Shao, J. Su, B. Ye, J.-X. Liu, Z.-L. Zuo, Y. Li, Y.-Y. Wang, C. Xia, Q.-S. Zhao, Design, Synthesis, and Biological Activities of Vibsanin B Derivatives: A New Class of HSP90 C-Terminal Inhibitors, J. Med. Chem. 60 (2017) 9053−9066.

[29]   Y. Wang, Y. Sun, R. Cao, D. Liu, Y. Xie, L. Li, X. Qi, N. Huang, In Silico Identification of a Novel Hinge-Binding Scaffold for Kinase Inhibitor Discovery, J. Med. Chem. 60 (2017) 8552−8564.

[30]   T. Okawa, Y. Aramaki, M. Yamamoto, T. Kobayashi, S. Fukumoto, Y. Toyoda, T. Henta, A. Hata, S. Ikeda, M. Kaneko, Design, synthesis, and evaluation of the highly selective and potent G-protein-coupled receptor kinase 2 (GRK2) inhibitor for the potential treatment of heart failure, J. Med. Chem. 60 (2017) 6942−6990.

[31]   J. A. Stefely, R. Palchaudhuri, P. A. Miller, R. J. Peterson, G. C. Moraski, P. J. Hergenrother, M. J. Miller, N-((1-Benzyl-1 H-1, 2, 3-triazol-4-yl) methyl) arylamide as a new scaffold that provides rapid access to antimicrotubule agents: synthesis and evaluation of antiproliferative activity against select cancer cell lines, J. Med. Chem. 53 (2010) 3389−3395.

[32]   J. A. Good, M. Kulén, J. Silver, K. S. Krishnan, W. Bahnan, C. Núñez-Otero, I. Nilsson, E. Wede, E. de Groot, Å. Gylfe, Thiazolino 2-pyridone amide isosteres as inhibitors of Chlamydia trachomatis infectivity, J. med. Chem. 60 (2017) 9393−9399.

[33]   Z. H. Chohan, M. Hanif, Design, synthesis, and biological properties of triazole derived compounds and their transition metal complexes, J. Enzyme Inhib. Med. Chem. 25 (2010) 737−749.

[34]   A. Kamal, N. V. S. Reddy, V. L. Nayak, N. R. Bolla, A. V. S. Rao, B. Prasad, Synthesis and evaluation of N-((1-benzyl-1H-1,2,3-triazol-4-yl)methyl)nicotinamides as potential anticancer agents that inhibit tubulin polymerization, Bioorg. Med. Chem. 22 (2014) 3465–3477.

[35]   Z.-H. Huang, S.-T. Zhuo, C.-Y. Li, H.-T. Xie, D. Li, J.-H. Tan, T.-M. Ou, Z.-S. Huang, L.-Q. Gu, S.-L. Huang, Design, synthesis and biological evaluation of novel
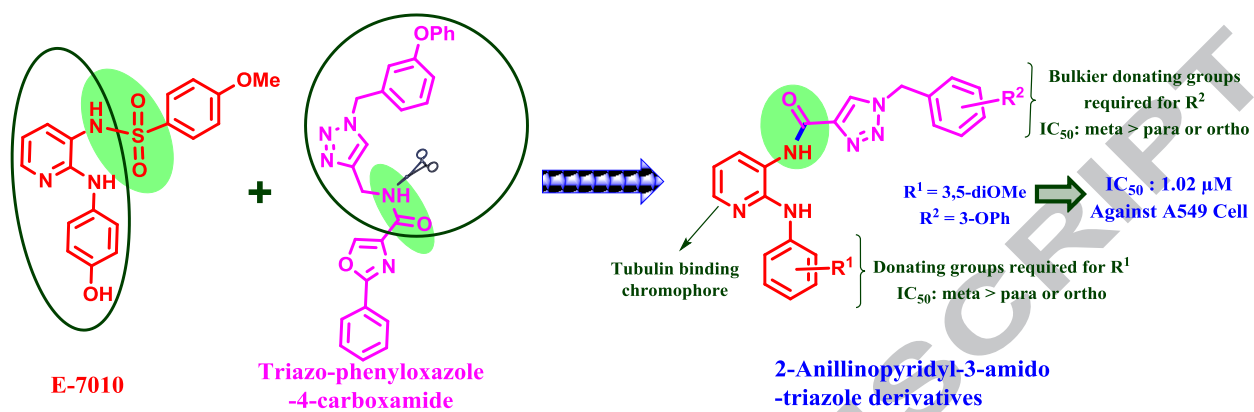
mansonone E derivatives prepared via CuAAC click chemistry as topoisomerase II inhibitors, Eur. J. Med. Chem. 68 (2013) 58−71.

[36]   S. G. Alvarez, M. T. Alvarez, A practical procedure for the synthesis of alkyl azides at ambient temperature in dimethyl sulfoxide in high purity and yield, Synthesis 1997 (1997) 413−414.

[37]   A. Kamal, N. S. Reddy, V. L. Nayak, N. R. Bolla, A. S. Rao, B. Prasad, Synthesis and evaluation of N-((1-benzyl-1H-1, 2, 3-triazol-4-yl) methyl) nicotinamides as potential anticancer agents that inhibit tubulin polymerization, Bioorg. Med. Chem. 22 (2014) 3465−3477.

[38]   F. Sultana, S. P. Shaik, V. L. Nayak, S. M. A. Hussaini, K. Marumudi, B. Sridevi, T. B. Shaik, D. Bhattacharjee, A. Alarifi, A. Kamal, Design, Synthesis and Biological Evaluation of 2- Anilinopyridyl- Linked Oxindole Conjugates as Potent Tubulin Polymerisation Inhibitors, Chem. Select, 2 (2017) 9901−9910.

[39]   (a) T. B. Shaik, S. M. A. Hussaini, V. L. Nayak, M. L. Sucharitha, M. S. Malik, A. Kamal, Rational design and synthesis of 2-anilinopyridinyl-benzothiazole Schiff bases as antimitotic agents, Bioorg. Med. Chem. Lett. 27 (2017) 2549–2558. (b) L. K. Mehta, J. Parrick, F. Payne, The Elimination of an Alkoxy Group in the Photo-Graebe-Ullmann Conversion of 1-(2,5- Dialkoxyphenyl)triazolopyridines into Carbolines, and the Preparation of a-,y- and 6-Carboline Quinones, J. Chem. Soc. Perkin Trans. 1, 0 (1993) 1261−1267. (c) S. -Li Cao, J. Zha, N. Zhang, Y. Wang, Y. –Y. Jiang, Y. –P. Feng, Synthesis and Crystal Structures of 4-(3-Nitropyridin-2- ylamino)phenol and 4-(3-Aminopyridin-2-ylamino)phenol, J. Chem. Crystallogr. 41 (2011) 1456–1460. (d) R. L. Clark, A. A. Pessolano, T. −Y. Shen, D. P. Jacobus, H. Jones, V. J. Lotti, L. M. Flataker, Synthesis and Analgesic Activity of 1,3-Dihydro-3-(substitutedphenyl)imidazo[4,5-blpyridin-2-ones and 3-(Substituted phenyl)-1,2,3-triazolo[4,5-blpyridines, J. Med. Chem. 21 (1978) 965−977.

[40]   (a) A. Kamal, B. Shaik, V. L. Nayak, B. Nagaraju, J. S. Kapure, M. Malik, T. B. Shaik, B. Prasad, Synthesis and biological evaluation of 1,2,3-triazole linked aminocombretastatin conjugates as mitochondrial mediated apoptosis inducers, Bioorg. Med. Chem. 22 (2014) 5155–5167. (b) V. G. Reddy, S. R. Bonam, T. S. Reddy, R. Akunuri, V.G.M. Naidu, V. L. Nayak, S. K. Bhargava, H.M. S. Kumar, P. Srihari, A. Kamal, 4β-amidotriazole linked podophyllotoxin congeners: DNA topoisomerase-IIa inhibition and potential anticancer agents for prostate cancer, Eur. J. Med. Chem 144 (2018) 595−611. (c) H.-b. Sun, D. Li, W. Xie, X. Deng, Catalytic cyclisation of 2,3-dibromopropionates with benzyl azides to afford 1-benzyl-1,2,3-triazole-4-carboxylate: The use of a nontoxic bismuth catalyst, Heterocycles, 92 (2016) 423−430.

[41]   K. T. Chan, F. Y. Meng, Q. Li, C. Y. Ho, T. S. Lam, Y. To, W. H. Lee, M. Li, K. H. Chu, M. Toh, Cucurbitacin B induces apoptosis and S phase cell cycle arrest in BEL-7402 human hepatocellular carcinoma cells and is effective via oral administration, Cancer lett. 294 (2010) 118−124.

[42]   C. Kanthou, O. Greco, A. Stratford, I. Cook, R. Knight, O. Benzakour, G. Tozer, The tubulin-binding agent combretastatin A-4-phosphate arrests endothelial cells in mitosis and induces mitotic cell death, The American J. pathology, 165 (2004) 1401−1411.

[43]   K. Huber, P.Patel, L. Zhang, H. Evans, A. D. Westwell, P. M. Fischer, S. Chan, S. Martin, 2-[(1-methylpropyl) dithio]-1H-imidazole inhibits tubulin polymerization through cysteine oxidation, Mol. Cancer Therap. 7 (2008) 143−151.

[44]   A. Kamal, Y.V.V. Srikanth, T. B. Shaik, M. N. A. Khan, M. Ashraf, M. K. Reddy, K. A. Kumar, S. V. Kalivendi, 2-Anilinonicotinyl linked 1, 3, 4-oxadiazole derivatives: Synthesis, antitumour activity and inhibition of tubulin polymerization, Med. Chem. Comm. 2 (2011) 819−823.

[45]   A. Kamal, P. Srikanth, M. Vishnuvardhan, G. B. Kumar, K. S. Babu, S. A. Hussaini, J. S. Kapure, A. Alarifi, Combretastatin linked 1, 3, 4-oxadiazole conjugates as a Potent Tubulin Polymerization inhibitors, Bioorg. Chem. 65 (2016) 126−136.

[46]   H. Zhu, J. Zhang, N. Xue, Y. Hu, B. Yang, Q. He, Novel combretastatin A-4 derivative XN0502 induces cell cycle arrest and apoptosis in A549 cells, Investigational New Drugs, 28 (2010) 493−501.

[47]   K. Gonda, H. Tsuchiya, T. Sakabe, Y. Akechi, R. Ikeda, R. Nishio, K. Terabayashi, K. Ishii, Y. Matsumi, A. A. Ashla, Synthetic retinoid CD437 induces mitochondria-mediated apoptosis in hepatocellular carcinoma cells, Biochem. Biophys. Res. Comm. 370 (2008) 629−633.

[48]   P. Srikanth, V. L. Nayak, K. S. Babu, G. B. Kumar, A. Ravikumar, A. Kamal, 2-Anilino-3-Aroylquinolines as Potent Tubulin Polymerization Inhibitors, ChemMedChem, 11 (2016) 2050−2062.

[49]   H. Wei, A. J. Ruthenburg, S. K. Bechis, G. L. Verdine, Nucleotide-dependent domain movement in the ATPase domain of a human type IIA DNA topoisomerase, J. Biolog. Chem. 280 (2005) 37041−37047.

[50]   G. M. Morris, R. Huey, W. Lindstrom, M. F. Sanner, R. K. Belew, D. S. Goodsell, A. J. Olson, AutoDock4 and AutoDockTools4: Automated docking with selective receptor flexibility, J. Comp. Chem. 30 (2009) 2785−2791.

[51]   W. L. DeLano, The PyMOL molecular graphics system. http://pymol. org. 2002.

[52]   M. Botta, S. Armaroli, D. Castagnolo, G. Fontana, P. Perad, E. Bombardelli, Synthesis and biological evaluation of new taxoids derived from 2-deacetoxytaxinine J, Bioorg. Med. Chem. Lett. 17 (2007) 1579−1583.

[53]   M. Szumilak, M. A. Szulawska, K. Koprowska, M. Stasiak, W. Lewgowd, A. Stanczak, M. Czyz, Synthesis and in vitro biological evaluation of new polyamine conjugates as potential anticancer drugs, Eur. J. Med. Chem. 45 (2010) 5744−5751.

[54]   K. Huber, P. Patel, L. Zhang, H. Evans, A. D. Westwell, P. M. Fischer, S. Chan, S. Martin, 2-[(1-methylpropyl) dithio]-1H-imidazole inhibits tubulin polymerization through cysteine oxidation, Mol. Cancer Ther. 7 (2008) 143–151.

 [55]   R. Shankar, B. Chakravarti, U. S. Singh, M. I. Ansari, S. Deshpande, S. K. D. Dwivedi, H. K. Bid, R. Konwar, G. Kharkwal, V. Chandra, A. Dwivedi and K. Hajela, Synthesis and biological evaluation of 3, 4, 6-triaryl-2-pyranones as a potential new class of anti-breast cancer agents, Bioorg. Med. Chem. 17 (2009) 3847–3856.

[56]   B. Chakravarti, R. Maurya, J. A. Siddiqui, H. K. Bid, S. M. Rajendran, P. P. Yadav, R. Konwar, In vitro anti-breast cancer activity of ethanolic extract of Wrightia tomentosa: role of pro-apoptotic effects of oleanolic acid and urosolic acid, J. Ethnopharm. 142 (2012) 72–79.

[57]   L.J. Browne, C. Gude, H. Rodriguez, R.E. Steele, A.J. Bhatnager, Fadrozole hydrochloride: a potent, selective, nonsteroidal inhibitor of aromatase for the treatment of estrogen-dependent disease, J. Med. Chem. 34 (1991) 725–736.

Graphical Abstract

E-7010

Triazo-phenyloxazole
-4-carboxamide

Tubulin binding
chromophore

Bulkier donating groups
required for R^2
IC_{50}: meta > para or ortho

R^1 = 3,5-diOMe
R^2 = 3-OPh

IC_{50} : 1.02 μM
Against A549 Cell

Donating groups required for R^1
IC_{50}: meta > para or ortho

2-Anillinopyridyl-3-amido
-triazole derivatives

Research Highlights:

➢ In the present studies, we have synthesized 1-Benzyl-N-(2-(phenylamino)pyridin-3-yl)-1H-1,2,3-triazole-4-carboxamide conjugates(**7a–7al**) were design, synthesized and evaluated for their cytotoxic activity against four human cancer cell lines.

➢ Among the synthesized conjugates **7a, 7b, 7c, 7f, 7h, 7j, 7m, 7n** exhibited good activity than standard **E7010** and possessing IC_{50} values < 1.6 μM against Human lung cancer cell line(A549).

➢ Conjugate **7f** have shown cytotoxic activity with IC_{50} value **1.023** μM againt Human lung cancer cell line(**A549**).

➢ These conjugates arrest cell cycle at G_2/M phase and molecular docking studies were performed which revealed the binding pose and explain the structural activity relationship of series.